

Genetic Types and Metallogenic Model for the Polymetallic Copper–Gold Deposits in the Tongling Ore District, Anhui Province, Eastern China



FU Zhongyang¹, XU Xiaochun^{1,*}, HE Jun¹, FAN Ziliang¹, XIE Qiaoqin¹, DU Jianguo² and CHEN Fang²

¹ School of Resources and Environmental Engineering, Hefei University of Technology, Hefei 230009, China

² Geological Survey of Anhui Province, Hefei 230001, China

Abstract: The Tongling ore district is one of the most economically important ore areas in the Middle–Lower Yangtze River Metallogenic Belt, eastern China. It contains hundreds of polymetallic copper–gold deposits and occurrences. Those deposits are mainly clustered (from west to east) within the Tongguanshan, Shizishan, Xinqiao, Fenghuangshan, and Shatanjiao orefields. Until recently, the majority of these deposits were thought to be skarn- or porphyry–skarn-type deposits; however there have been recent discoveries of numerous vein-type Au, Ag, and Pb–Zn deposits that do not fall into either of these categories. This indicates that there is some uncertainty over this classification. Here, we present the results of several systematic geological studies of representative deposits in the Tongling ore district. From investigation of the ore-controlling structures, lithology of the host rock, mineral assemblages, and the characteristics of the mineralization and alteration within these deposits, three genetic types of deposits (skarn-, porphyry-, and vein-type deposits) have been identified. The spatial and temporal relationships between the orebodies and Yanshanian intrusions combined with the sources of the ore-forming fluids and metals, as well as the geodynamic setting of this ore district, indicate that all three deposit types are genetically related each other and constitute a magmatic–hydrothermal system. This study outlines a model that relates the polymetallic copper–gold porphyry-, skarn-, and vein-type deposits within the Tongling ore district. This model provides a theoretical basis to guide exploration for deep-seated and concealed porphyry-type Cu (–Mo, –Au) deposits as well as shallow vein-type Au, Ag, and Pb–Zn deposits in this area and elsewhere.

Key words: polymetallic copper–gold deposits, genetic types, metallogenic model, magmatic–hydrothermal system, Tongling ore district, Anhui Province

Citation: Fu et al., 2019. Genetic Types and Metallogenic Model for the Polymetallic Copper–Gold Deposits in the Tongling Ore District, Anhui Province, Eastern China. *Acta Geologica Sinica* (English Edition), 93(1): 88–110. DOI: 10.1111/1755-6724.13635

1 Introduction

The Middle–Lower Yangtze River Metallogenic Belt (MLYB) is a well-known metallogenic belt in eastern China that contains more than 200 polymetallic Cu–Fe–Au–Mo deposits (Chang Yinfo et al., 1991; Pan and Dong, 1999; Deng et al., 2011; Mao et al., 2006, 2011; Zhou Taofa et al., 2012; Xie Guiqing et al., 2013; Zhou et al., 2014; Cao et al., 2015; Duan et al., 2018). It extends from Wuhan (Hubei Province) in the west to Zhenjiang (Jiangsu Province) in the east, and comprises the following seven ore districts: Edong, Jiurui, Anqing–Guichi, Tongling, Luzong, Ningwu and Ningzhen. Evaluation of their genetic types and creation of an accurate metallogenic model for ore deposits are still research hotspots in the MLYB, about which hundreds of scientific papers have been published. The Tongling ore district is one of the economically most important polymetallic copper–gold mining districts in the belt (Deng et al., 2011; Xu et al., 2011; Qu et al., 2012; Duan et al., 2017). It is located in an

uplifted area that contains voluminous intermediate–acid intrusions and numerous associated polymetallic copper–gold deposits (Chang Yinfo et al., 1991; Xie et al., 2009; Zhou Taofa et al., 2009; Deng et al., 2011; Mao et al., 2009; Wang et al., 2011; Xu et al., 2011). A significant amount of previous research has been undertaken in this area since the 1950s, focusing on the Tongguanshan, Shizishan, Xinqiao, Fenghuangshan, and Shatanjiao orefields. This activity has made the area one of the best known ore districts in the world, for skarn-type deposits (Huang Chongke et al., 2001; Zhang et al., 2017). For example, the polymetallic copper–gold deposits within the Tongling ore district were originally interpreted as typical skarn-type deposits (Guo Wenkui, 1957; Guo Zongshan, 1957; Zhao Bin, 1989). The orebodies mainly occur in contact zones between the Yanshanian intrusions and carbonate rocks, where the skarn mineral assemblages are well-developed. Chang Yinfo and Liu Xuegui (1983) proposed a stratabound–skarn model for these deposits, based on the hosting of orebodies by carbonate rock at the base of the Carboniferous Huanglong and Chuanshan Formations. The later identification of magmatic minerals

* Corresponding author. E-mail: xuxiaoch@sina.com

within these skarns led to the outlining of a magmatic–skarn model (Wu Yanchang et al., 1992, 1996, 1998). Although some research had suggested that deposits (such as Dongguashan and Xinqiao deposits) were formed by syngenetic sedimentation (Meng Xianmin et al., 1963; Zhai Yusheng et al., 1992), or resulted from superimposition of Yanshanian magmatic mineralization on the Hercynian synsedimentary massive sulfides (Xu Keqin and Zhu Jinchu, 1978; Gu Lianxing and Xu Keqin, 1986; Zeng Pusheng et al., 2005; Xu Zhaowen et al., 2007; Lu Jianjun et al., 2008; Hou Zengqian et al., 2011), the skarn-type model for the mineralization was still generally accepted. It should also be noted that the skarn-type deposits within the Shizishan orefield have different forms, including stratabound, contact, interlayer, fissure, and crypto-explosive breccia styles of mineralization, leading to the outlining of a multi-position pattern for these different styles of skarn mineralization (Chang Yinfo et al., 1991).

Porphyry-type deposits were scarcely found in this area before 21st century. But in recent decade, many new porphyry Cu (Au) deposits, such as Shujiadian (Wang et al., 2014) and Guihuachong Cu (Au) deposit (Yue Zilong, 2015), have been discovered. Thus porphyry-type deposits have gained more and more attention in the Tongling ore district. Some porphyry mineralization developed at depth below the skarn mineralization, such as the Dongguashan and Hucunnan porphyry–skarn deposits (Yuan Feng et al., 2014; Zheng Zejun et al., 2015; Wang et al., 2015). This led to definition of a porphyry–skarn system (Mao Jingwen et al., 2009; Yuan Feng et al., 2014). With continuous prospecting work, however, this area also contains numerous, but generally small, vein-hosted Au, Ag, and Pb–Zn deposits. These are always located at shallow depths relative to other mineralization (e.g., the Jiaochong polymetallic deposit; Zhang Zhihui et al., 2013). These discoveries have revealed a new Au–Ag–Pb–Zn potential in the Tongling ore district. The geologic features of these deposits are neither similar to skarn-type nor to porphyry-type deposits, leading Xu Xiaochun et al. (2014) to classify them as epithermal hydrothermal deposits. According to field investigations of these deposits and a detailed study of the date available, we prefer to use the term “vein-type” (Edwards and Atkinson, 1986) for these deposits, and details of their distinctive characteristics will be discussed in later sections.

Overall, although a significant amount of research has been undertaken in the study area over the last 60 years, the majority has focused on skarn-type or porphyry-type mineralization. The genetic type of these vein-hosted deposits is still unclear, and the genetic relationships between these three deposit types require further examination as well. For this paper we reviewed the Tongling ore district in some detail, documented the essential characteristics of the polymetallic copper–gold deposits, and highlighted a few examples of vein-type mineralization. Herein, we also discuss time–space distribution between orebodies and intrusions, as well as the sources of the fluids that formed the ore in these deposits.

2 Regional Geological Setting

The Tongling ore district lies in the middle part of the MLYB at the northern margin of Yangtze Craton (Chang Yinfo et al., 1991; Tang Yongcheng et al., 1998; Pan and Dong, 1999). This area records three periods of tectonism, comprising basement formation during the Mesoproterozoic–Neoproterozoic Pre-Nanhua period, cover layers during the Neoproterozoic Nanhua period to Early Triassic Era, and the Middle–Late Triassic to the Cenozoic Era of collisional orogeny and associated post-orogenic intraplate deformation, respectively (Ma Xingyuan and He Guoqi, 1989; Wang Hongzhen and Mo Xuanxue, 1995). The area was subjected to multiple tectonic movements, which were characterized by a series of prominent Mesozoic NE–SW-trending S-folds. From west to east, the area was affected by the Tongguanshan anticline, Shun’an synclinorium (the Taojiacun syncline + Qinshan anticline + Zhucun syncline), Shujiadian–Yongcunqiao anticline, Fenghuangshan synclinorium (the Fenghuangshan syncline + Xianrenchong anticline + Yuanbaoshan syncline) and the Daigongshan anticline (Li Wenda, 1989; Liu Wencan and Li Dongxu, 1993; Wang et al., 2010; Deng et al., 2011). Besides, Yanshanian NE–SW and NNE–SSW-trending folds are commonly superimposed on the E–W-trending ones (Liu Wencan and Li Dongxu, 1993). There also are a number of fault networks that include deep-seated and basement-penetrating faults that are divided into E–W, N–S, and NNE–SSW trending groups within the cover sequence (Chu Guozheng and Li Dongxu, 1992; Liu Wencan et al., 1996; Wu Ganguo et al., 2003). These structural frameworks control the location of both magmatism and related hydrothermal fluid activity (Wang et al., 2010; Deng et al., 2011). Stratigraphic sequences in the Tongling ore district outcrops are dominated of Silurian to Cretaceous sedimentary units that have a total thickness of as much as to 4500 m. The Upper Carboniferous–Lower Permian Huanglong and Chuanshan Formations, Middle Permian Qixia Formation, Upper Permian Dalong Formation, and Lower Triassic Yinkeng, Helongshan, and Nanlinghu Formations are ore-bearing horizons. More than 76 intrusions outcrop in a wide area along the E–W trending Tongling–Shatanjiao tectono-magmatic belt, with formation ages mainly in the range of 135–147 Ma (Xing Fengming and Xu Xiang, 1996; Xing Fengming et al., 1997; Pan and Dong, 1999; Xu Xiaochun et al., 2012; Wu Cailai et al., 2013; Du et al., 2015). These intrusions are dominated by pyroxene diorite, quartz diorite, and granodiorite lithologies, all of which are genetically associated with mineralization (Xie et al., 2009; Wang et al., 2010; Deng et al., 2011; Xu Xiaochun et al., 2012). More than a hundred ore deposits have been identified along the Tongling–Shatanjiao tectono-magmatic belt, and these exhibit a zonal distribution, i.e., the Cu–(Mo, Au) deposits are found at the middle part, while the polymetallic (Au, Ag, and Pb–Zn) mineralization exists at the sides (Fig. 1). These ore deposits are mainly clustered in the Tongguanshan, Shizishan, Fenghuangshan, Xinqiao, and Shatanjiao orefields (Fig. 1). These orefields contain >5 million tons of Cu, >100 tons of Au, as well as

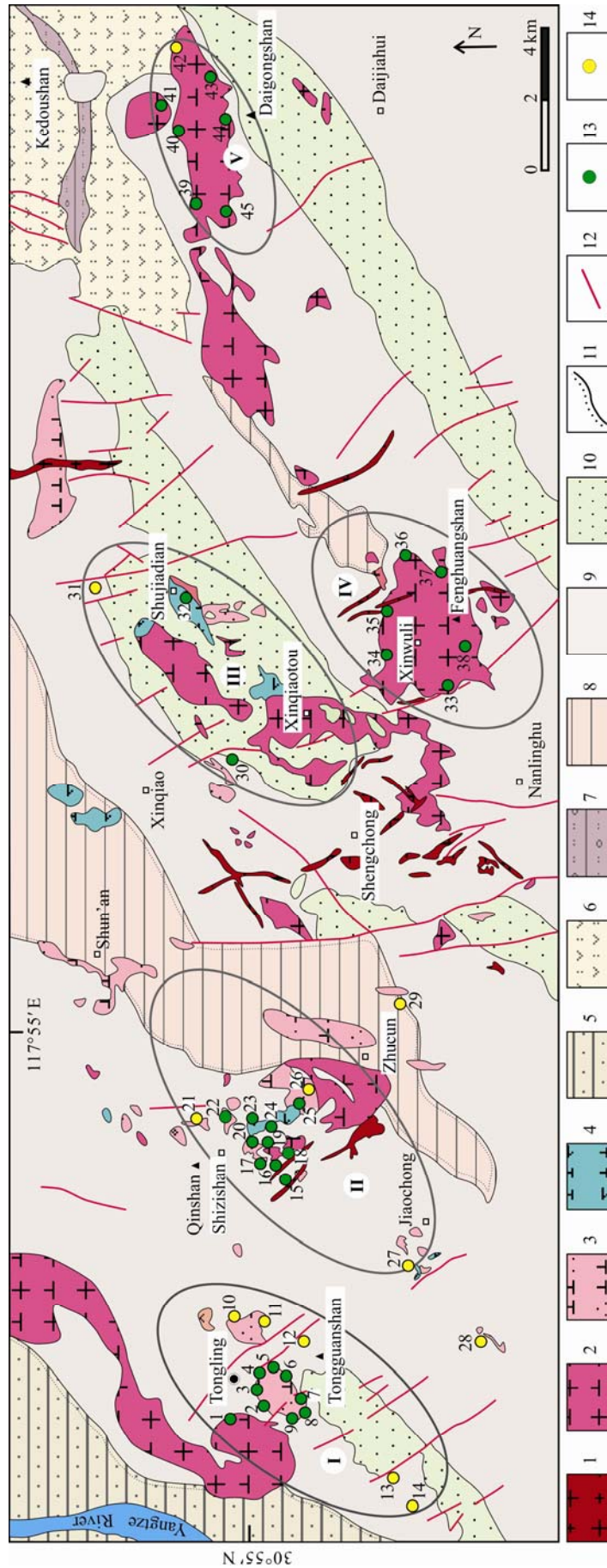


Fig. 1. Distribution of the polymetallic copper–gold deposits in the Tongling ore district, Anhui Province modified (from Xu Xiaochun et al., 2012).

significant amounts of Ag, Pb, Zn, Mo, and Fe (Wu Cailai et al., 2010), although single ore deposit typically only contains 0.5–1 million tons of Cu or less.

3 Geology of the Polymetallic Copper–Gold Deposits

Both skarn-type and porphyry-type mineralization are generally accepted in the study area. The former is the most economically significant type of mineralization, and is represented by the large Tongguanshan Cu, Dongguashan Cu–Au, Xinqiao Cu–Au–S and Fenghuangshan Cu deposits. A significant amount of previous research has been undertaken in those deposits. The latter is found mainly within intrusive body at deep-seated of the Dongguashan and Hucunnan deposit. Besides, Shujiadian Cu deposit is one of the most representative porphyry-type deposits in this area. Comparatively speaking, studies on vein-type mineralization are still rare. Due to this mineralization usually overprinted skarn- or porphyry-type mineralization, the identification of vein-type deposits is more difficult. The vein-type mineralization is also great potential, although they are generally of smaller scale of mineralization. Along with the large or medium size vein-hosted Au, Ag, and Pb–Zn deposits discovery such as the Yaojialing, Jiaochong and Baocun, the great progress has been made in prospecting for this area.

This section outlines the key geological and metallogenic features in the Tongling ore district and describes several representative deposits (i.e., Dongguashan, Hucunnan, Jiaochong, Yaojialing, Hehuashan and Baocun deposits). The main characteristics of the representative deposits are listed in Table 1 and

their locations are shown in Fig. 1.

3.1 Skarn and porphyry deposits

The Dongguashan and Hucunnan are typical porphyry–skarn deposits in the Tongling ore district (Xu Xiaochun et al., 2008; Xu et al., 2011; Liu Zhongfa et al., 2014; Yuan Feng et al., 2014; Wang et al., 2015; Zheng Zejun et al., 2015; Yang et al., 2016).

Dongguashan, the first large Cu–Au deposit in the Shizishan orefield, lies about 8 km east of Tongling City (Fig. 1). The Cu–Au mineralization is divided into a shallow stratabound skarn-type deposit and a deeper porphyry-type deposit (Xu Xiaochun et al., 2014; Wang et al., 2015). It holds Cu reserves of 1 Mt and Au reserves of 25 t (Zeng Pusheng et al., 2005). The rock that outcrops in the Dongguashan area is mainly limestone of the Lower Triassic Nanlinghu and Helongshan Formations, as well as apophyse-like intrusions of Baocun and Qingshanjiao quartz diorites (Fig. 2a). The latter is associated with the deposits, outcrops at the surface over an area of $\sim 0.2 \text{ km}^2$, and has yielded a SHRIMP zircon U–Pb age of $135.5 \pm 2.2 \text{ Ma}$ (Xu Xiaochun et al., 2008).

The upper stratabound skarn-type mineralization takes place at dolomites or dolomitic limestones of the Upper Carboniferous Huanglong and Chuanshan Formations (Fig. 2b). More than 138 Cu orebodies have been recognized, of which the length and thickness of the main Cu orebody is typically about 3000 m and 1–100 m, respectively (Pan and Dong, 1999; Huang Chongke et al., 2001). The orebodies usually have a stratiform shape (Figs. 2b and 3a) and are constrained by the stratigraphic horizon, fold structure, and interlaminar décollement structure. The ore types within the deposit are

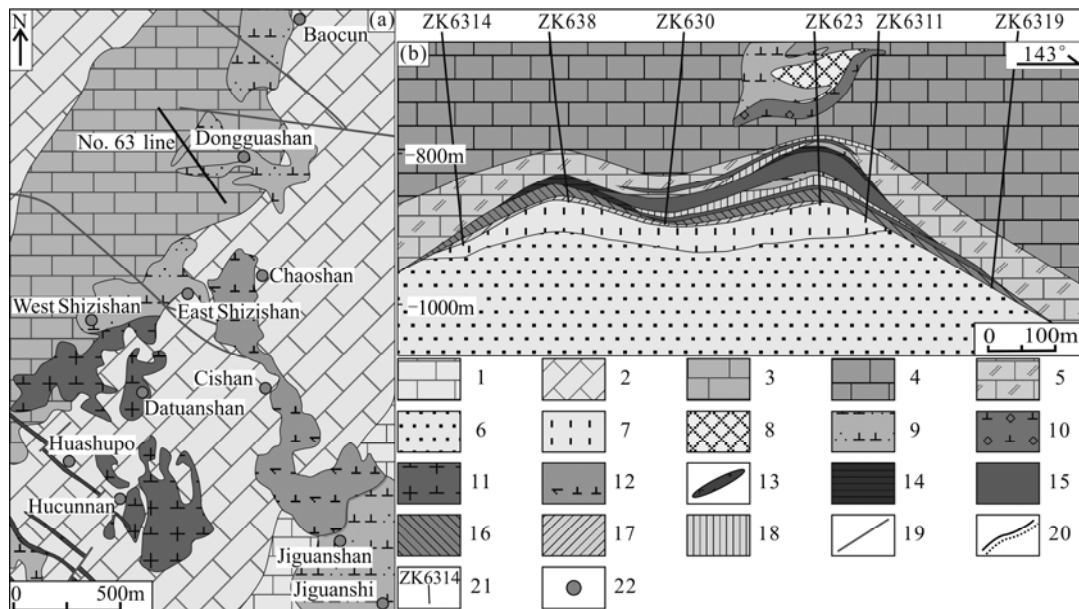


Fig. 2. Geological sketch map of the Shizishan orefield (a) and cross-section of No. 63 line of the main orebody in the Upper Dongguashan Cu–Au deposit (b) (modified from Xu et al., 2011; Xu Xiaochun et al., 2014).

1, Middle Triassic Dongma'anshan Formation; 2, Lower Triassic Nanlinghu Formation; 3, Lower Triassic Helongshan Formation; 4, Lower Permian Qixia Formation; 5, Carboniferous Huanglong–Chuanshan Formation; 6, Upper Devonian Wutong Formation; 7, silicified sandstones; 8, skarn; 9, quartz diorite; 10, skarn-altered quartz diorite; 11, granodiorite; 12, pyroxene diorite; 13, granite–porphyry dyke; 14, Cu-bearing anhydrite ore; 15, Cu-bearing pyrrhotite–pyrite ore; 16, Cu-bearing pyrite–serpentinite ore; 17, Cu-bearing hornfel ore; 18, Cu-bearing skarn ore; 19, faults; 20, observed/inferred geological boundary; 21, drill holes and number; 22, deposits.

Table 1 Characteristics of typical polymetallic copper-gold deposits in the Tongling ore district, Anhui Province

Deposit	Type	Orebody morphology	Main host rocks	Ore-controlling structure	Main Hydrothermal alteration	Main ore types	Main ore mineral	Main gangue mineral	Ore forming temperature (°C)	Ref.
Upper Dongguashan	skarn	stratiform	carbonate rocks	interlaminar décollement structure	skarn, serpentine, carbonate	Cu-bearing skarn, serpentinite, pyrrhotite ores	Po, Py, Ccp, Mag, Gl, Sp	Di, Adr, Srp, Tlc, Anh, Qtz, Cal	220–548	1
Deeper Dongguashan	porphyry	lens-shaped	quartz diorite	fissure of f intrusive body	K-feldspar, quartz-sericite, propylite	Cu-bearing quartz diorite ores	Py, Po, Ccp, Mo, Mag, Gn, Sp, Gl	Kfs, Chl, Ser, Anh, Qtz, Cal	347–588	2
Upper Huocunman	skarn	lens-shaped, thin-sheet	granodiorite, limestone	intrusive contact structure	skarn, chlorite, carbonate, epidote	Cu-bearing skarn ores	Ccp, Po, Py, Mo, Sp, Gn	Grt, Di, Qtz, Cal, Chl, Ep, Kfs, Bt, Ser,	203–570	3
Deeper Huocunman	porphyry-skarn	lens-shaped	granodiorite, silicite, limestone	fissure of f intrusive body	K-feldspar, quartz-sericite, chlorite, epidote	Cu/Mo-bearing granodiorite ores	Mo, Py, Po, Ccp		282–52	4
Shuijiadian	porphyry	lens-shaped	pyroxene diorite	fissure of intrusive body	K-feldspar, quartz-sericite, chlorite, epidote	Cu-bearing pyroxene diorite ores	Ccp, Py, Po, Mot, Mag, Hem	Px, Qtz, Kfs, Pl, Am, Bt	291–600	5
Tongguanshan	skarn	lens-shaped, tabular, saccular, stratoid	quartz diorite, carbonate rock	intrusive contact structure	skarn, carbonate, serpentine, chlorite	Cu-bearing skarn, serpentinite, pyrrhotite ores	Po, Mag, Ccp, Py	Grt, Di, Srp, Tlc, Chl, Qtz, Cal		6
Yaoyuanshan	skarn	lens-shaped, thin-sheet	quartz diorite, carbonate rocks	intrusive contact structure	skarn, carbonate, poash feldspar, chlorite, epidote, sericite	Cu-bearing skarn, quartz diorite, marble ores	Ccp, Bn, Mag, Py	Qtz, Cal, Adr, Di, Chl, Pl	210–594	7
Baocun	skarn	lens-shaped	quartz diorite, limestone	intrusive contact structure	skarn, carbonate, poash feldspar, chlorite, epidote	Au (Cu)-bearing skarn ores	Py, Ccp, Po, Gl	Grt, Di, Qtz, Cal, Chl	253–478	8
	vein	vein-hosted	limestone	fracture	marble, quartz, pyrite	Au-bearing breccia, pyrite and Au (Bi)-bearing quartz veins	Gl, Bi, Py, Ccp	Qtz, Cal	198–278	
Jiaochong	vein	stratiform, vein-hosted	limestone, marble	interlaminar fracture of limestone	skarn, marble, quartz, pyrite	massive, vein-type ores	Po, Py, Sp, Gn, Mag, Gl	Qtz, Cal	200–390	4
Jiguanshi	vein	vein-hosted, lens-shaped	Dolomitic marble	fracture	skarn, quartz, pyrite	Au-bearing pyrite, breccia, marble ores	Slv, Gl, Pb, Sp, Py	Qtz, Cal	150–300	9
	porphyry	lens-shaped	granodiorite porphyry	fissure of intrusive body	K-feldspar, quartz-sericite, chlorite	porphyry-type ores		Pl, Bt, Ser, Kln		
Yaotaijing	skarn	lens-shaped	Limestone, granodiorite porphyry	intrusive contact structure	skarn;	skarn-type ores;	Sp, Ccp, Gn, Hem, Mag, Py	Di, Grt, Ep, Chl, Qtz, Cal, Dol	160–420	10
	vein	lens-shaped, vein-hosted	limestone	interlaminar fracture of limestone	carbonate, quartz, pyrite;	massive, vein-type ores;	Py, Sp, Ccp, Gn	Qtz, Cal		

Note: 1, Liu Zhongfa et al., 2014; 2, Wang Shiwei, 2015; 3, Zheng Zejun et al., 2015; 4, this paper; 5, Wang et al., 2014; 6, Zhou Taofa et al., 2009; 7, Qu Hongying et al., 2011; 8, Ren Yunsheng et al., 2006; 9, Chu Guozheng, 2003; 10, Wen Chunhua et al., 2011

Mineral abbreviation: Bn-bornite; Ccp-chalcopyrite; Gl-native gold; Gn-galena; Hem-hematite; Mag-magnetite; Mo-molybdenite; Po-pyrrhotite; Py-pyrite; Slv-native silver; Sp-sphalerite; Adr-andradite; Am-amphibole; Anh-anhydrite; Brt-barite; Bt-biotite; Cal-calcite; Chl-chlorite; Di-diopside; Dol-dolomite; Grt-garnet; Kfs-K-feldspar; Kln-kaolinite; Pl-plagioclase; Px-pyroxene; Qtz-quartz; Ser-sericite; Srp-serpentine; Tlc-talc

complicated, but skarn-type mineralization is predominant (Fig. 3c), with small amounts of Cu-bearing quartz diorite ores. Metallic minerals in the ore assemblages are mainly pyrrhotite, pyrite, chalcopyrite, magnetite, electrum, and native gold with minor amounts of cubanite, sphalerite, siderite and marcasite. The gangue minerals are predominantly andradite, diopside, tremolite, serpentine, talc, anhydrite, quartz, and calcite. All of them appear massive, although disseminated in structure. Wrigglite and laminated ores are also common (Fig. 3d). The deposit has undergone intense contact metamorphism and hydrothermal alteration that has generated skarn (Fig. 3c and e), serpentinite (Fig. 3f), chlorite (Fig. 3f), talc, carbonate and anhydrite alteration. Skarn mineral assemblages include andradite, diopside–salerite, actinolite–tremolite, wollastonite, and epidote along with magnesium

skarn minerals such as olivine and exhibit later hydrothermal retrograde metamorphism that produced serpentine and talc (Fig. 3f).

The deep-seated part of the Dongguashan system is a porphyry-type deposit located beneath the skarn mineralization. Two lens-shaped major orebodies are situated in the Baocun and Qingshanjiao quartz diorite intrusions and their contact zones at depths of –890 to –1010 m. They consist of veins, veinlets-stockworks and disseminations of chalcopyrite, pyrite and pyrrhotite, as well as minor amounts of molybdenite, magnetite, galena and sphalerite (Fig. 3b and g–h). The ore-bearing intrusions developed extensive hydrothermal alteration and zones from the center of the deposit outwards in the following order: quartz–K-feldspar (Fig. 3i), quartz–sericite (Fig. 3i–j), propylitic (Fig. 3i–k), skarn (Fig. 3e),

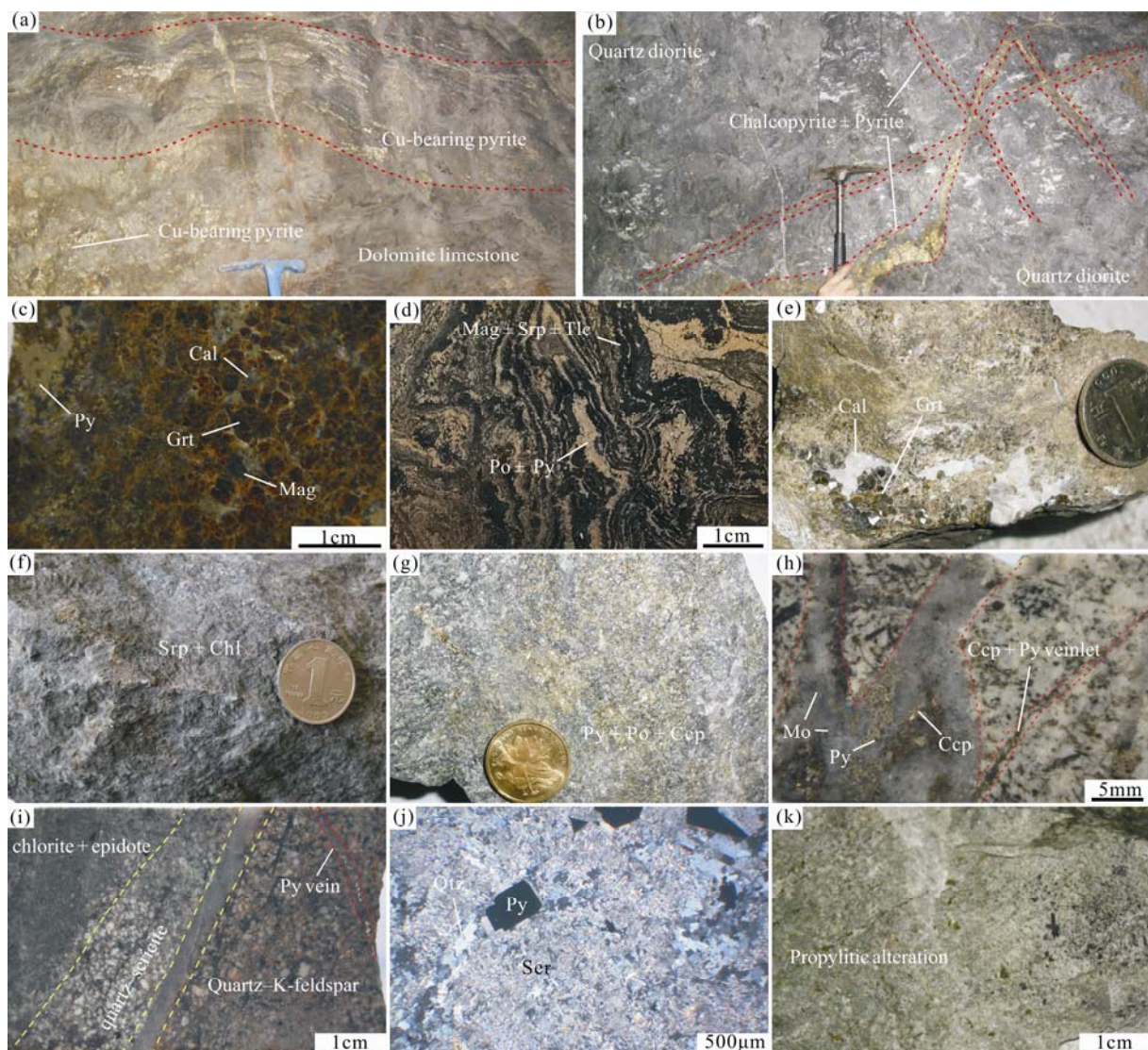


Fig. 3. Photographs showing mineralization and alteration characteristics of the Dongguashan deposit.

(a) stratiform Cu-bearing pyrite sulfide orebody; (b) Cu-bearing quartz veinlets and stockworks which developed in quartz diorite; (c) skarn-type ore consists of magnetite, pyrite and minor calcite within garnet skarn; (d) wrigglite and laminated ore consists of the pyrrhotite, pyrite, magnetite, talc and serpentine interbed; (e) quartz diorite with intensive skarn alteration, idiomorphic or hypidiomorphic granular garnet together with calcite; (f) skarn is pervasively replaced by serpentine and overprinted by later chlorite; (g) Cu-bearing quartz diorite ore with disseminated chalcopyrite, pyrrhotite and pyrite; (h) chalcopyrite–pyrite–molybdenite–quartz vein and veinlet cut through quartz diorite; (i) pervasive quartz–K-feldspar alteration quartz diorite, overprinted by later quartz–sericite and propylitic alteration; (j) pervasive pyrite–sericite–quartz alteration in quartz diorite (plane-polarized light of microphoto); (k) propylitic alteration consisting of epidote, chlorite, quartz, carbonate and pyrite.

marble alteration, and then development of a hornfels zone. Mineralization is well developed in the K-feldspar alteration zone, whereas the quartz–sericite alteration zone is essentially barren (Tang Yongcheng et al., 1998).

The Hucunna Cu–Mo–(Au) deposit is located some 2 km southwest of the Dongguashan deposit (Figs. 1 and 2a; Chang Yinfo et al., 1991; Zheng Zejun et al., 2015; Yang et al., 2016; Cao et al., 2017). It is a newly discovered porphyry-skarn deposit, which represents a shallow Cu–(Au) dominant skarn system that is underlain by a deeper Cu–Mo dominated porphyry–skarn system (Fig. 4a–b; Xu Xiaochun et al., 2011; Fan Ziliang et al., 2016). Intrusive rock outcropped in this deposit is the ore-associated Hucunna granodiorite stock, which outcrops over an area of 0.35 km², and has a zircon SHRIMP U–Pb age of 140.0±2.6 Ma (Fig. 2a; Xu Xiaochun et al., 2008).

The upper part of Hucunna deposit was discovered in the 1990s, and extends from 300–600 m below the surface (Xu Xiaochun et al., 2008). It is a classic skarn deposit (Chang Yinfo et al., 1991; Zhai Yusheng et al., 1992; Xu Xiaochun et al., 2011; Cao et al., 2017). The main orebody has a lens or tabular shape and is situated in contact zones between the granodiorite and country rock (Fig. 4a). The ore types in the deposit are represented by Cu-bearing skarn, massive ores and small amounts of Cu-bearing granodiorite. And sulfide ores are typically massive, disseminated, or vein-hosted. Ore metallic minerals mainly include chalcopyrite, pyrrhotite, and pyrite, with minor amounts of molybdenite, sphalerite and galena, etc. Gangue minerals are represented by garnet, diopside, epidote, chlorite, quartz and calcite. Intense contact

metamorphism and hydrothermal alteration generated skarn, chlorite, carbonate, and epidote alteration. The alteration zonation is very distinctive, which follows the sequence: skarnification of the granodiorite → inner skarn → massive skarn → bedded skarn → marble or hornfels zone (Chu Guozheng, 2003).

The deep-seated part of Hucunna deposit was proven to be a porphyry–skarn deposit (Xu Xiaochun et al., 2008; Zheng Zejun et al., 2015; Yang et al., 2016). It is located at depths of >1000 m from the surface and was discovered comparatively recently. The skarn-type orebodies are present as lenses or as bedded mineralization within interlaminar fractures of the Qixia Formation limestone and silicalite (Fig. 4b). The mineralization, ore types and alteration characteristics are similar to those present in the overlying skarn deposit. In contrast, the underlying porphyry-type orebodies are generally lens-like and hosted in granodiorite intrusion and its contact zones (Fig. 4b). The Cu (Mo) mineralization is characterized by Cu- or Mo-bearing quartz veinlets and stockworks which developed in granodiorite, with minor disseminated mineralization distributed locally. Ore minerals mainly include chalcopyrite, molybdenite, pyrite and pyrrhotite, gangue minerals are mainly quartz, feldspar, hornblende, and minor biotite, chlorite, and sericite. The Wall rock alteration in the deep granodiorite intrusion is extensive and also shows a well-defined alteration zoning from center outward: potassic alteration (K-feldspar + quartz ± biotite) → pyritized-phyllite alteration (sericite + quartz + minor pyrite) → propylitic alteration (chlorite + epidote ± calcite ± quartz) → skarn zone.

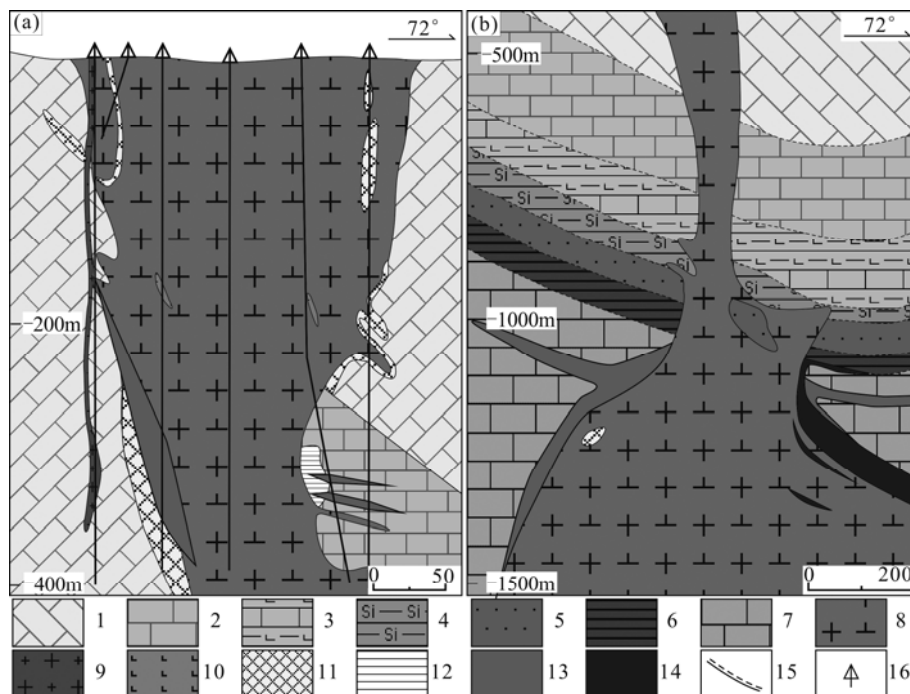


Fig. 4. Cross-section of the main orebody in the Upper Hucunna Cu–Au deposit (a) and Lower Hucunna Cu–Mo deposit (b) (modified from Xu Xiaochun et al., 2014).

1, Lower Triassic Nanlinghu Formation; 2, Lower Triassic Helongshan Formation; 3, Lower Triassic Yinkeng Formation I; 4, Upper Permian Dalong Formation; 5, Upper Permian Longtan Formation; 6, Lower Permian Gufeng Formation; 7, Lower Permian Qixia Formation; 8, granodiorite; 9, granite porphyry; 10, odinite; 11, skarn; 12, marble with intercalation of hornfels and skarn; 13, Cu orebodies; 14, Mo orebodies; 15, observed/inferred geological boundary; 16, drill holes.

3.2 Vein-type deposits

3.2.1 Jiaochong polymetallic deposit

The Jiaochong deposit is a recently discovered polymetallic Au–S deposit located within the SE limb of the Qingshan anticline, about 8 km southeast of Tongling City (Fig. 1). This area contains limestones and marbles of the Middle Triassic Nanlinghu and Dongmaanshan Formations, as well as of Lower Triassic Helongshan Formation limestones and calcareous shales (Fig. 5a; Zhang Zhihui et al., 2013; Zhang Shoucheng and Zhao Yan, 2016). The faults are well developed and three phases of faults may be distinguished. These include the initial development of NE–SW trending interlaminar décollement structures, followed by the development of NE–SW and NW–SE trending faults and a final phase of sinistral strike-slip faults in the southern part of this area (Zhang Zhihui, 2009). The early NE-trending interlaminar décollement structures are thought to provide the space that allowed the deposit to form (Zhang Shoucheng and Zhao Yan, 2016). The intrusive rocks are mainly ore-associated pyroxene diorite, as well as diorite and dioritic porphyrite stocks (Que Chaoyang et al., 2013; Du Jingguo et al., 2016).

The mineralization is located at depths of –370 to –830 m. Three Au–S or Pb–Zn orebodies have been recognized in this area, typically with length and thickness of 40–120 m and 0.80–19.18 m, respectively. The main orebody is both stratiform and vein-shaped and is entirely hosted within Permian Qixia Formation limestones (Fig. 5b). Its overlying hanging wall is formed by Qixia Formation silicalites and the footwall of the deposit is dominated by marble. The ore types in the deposit are represented by massive (Fig. 6a) or vein-type ores (Fig. 6b–c), although some taxitic and disseminated ores (Fig. 6d) are also present. Metallic minerals in the ore assemblages are mainly pyrrhotite, pyrite, sphalerite, and native gold, with lesser amounts of galena, arsenopyrite, electrum, chalcopyrite, and magnetite. Quartz and calcite are primary components of the gangue, which also contains small amounts of feldspar, actinolite, tremolite, wollastonite, garnet, fluorite, sericite, and chlorite.

The Jiaochong deposit is associated with significant wall rock hydrothermal alteration, including the metamorphism of Carboniferous–Triassic carbonates to form marbles or marble-altered limestones (Fig. 6c–e) and the development of hornfels units within the shales and silicalite. The contact zone between the intrusive rock and the surrounding limestone is generally skarn altered (Fig. 6f), and the intrusion is surrounded by zones of alteration from unaltered rocks through to garnet skarn and skarn-altered marble zones to a distal marble zone. The intrusive rocks have also undergone weak chlorite, kaolin, K-feldspar, and sericite alteration, as well as silicification. However, the mineralization of this deposit is poorly associated with skarn alteration, as exemplified by the fact that neither contact nor skarn zones contain orebodies (Fig. 6f). Instead, the orebodies that define the deposit are controlled by both interlaminar décollement structures and fractures within the limestone units. The majority of the latter are located within layer-parallel fractures of the Qixia Formation limestones (Figs. 5b and 6b–e). The ores

commonly occur as massive or disseminated sulfides within marble-altered limestones (Fig. 6a and d), or occur as vein-shaped and filling in interlayer fractures of marble and marble-altered limestone units (Fig. 6b–c). They may also occur as massive sulfide ores in close contact with the surrounding marble-altered limestones (Fig. 6b and e). All of these indicate that the Jiaochong deposit is a vein-type deposit (Zhang Zhihui et al., 2013; Zhang Shoucheng and Zhao Yan, 2016).

3.2.2 Yaojialing polymetallic deposit

The Yaojialing polymetallic deposit is located within the eastern margin of the Tongling ore district (Fig. 1; Jiang Qisheng et al., 2005, 2008; Wen Chunhua et al., 2011; Zhong Guoxiong et al., 2014; Yin Yanduan et al., 2016) and is the largest porphyry–skarn–vein-type deposit within the Shatanjiao orefield (Liu Shaofeng, 2012). Here we mainly focused on its vein-type mineralization.

The southern part of the Yaojialing area contains sandstone, siltstone, shale units of the upper Silurian Maoshan and Upper Devonian Wutong Formations, whereas the eastern and central parts of the area contain Carboniferous to Middle–Lower Triassic carbonate and the northern parts of the area contains terrestrial facies clastic and pyroclastic units of the Lower Cretaceous Kedoushan Formation (Fig. 7a; Jiang Qisheng et al., 2008). The mineralization-associated Yaojialing granodiorite porphyry stock was emplaced into units within the northwestern limb of the Daigongshan anticline and is 1800 m long, 300–500 m wide, and outcrops over an area of ~0.75 km² (Jiang Qisheng et al., 2005, 2008). Drilling in this deposit has identified widespread cryptoexplosive breccias as well as numerous Carboniferous to Permian limestone xenoliths within the Yaojialing granodiorite porphyry (Wen Chunhua et al., 2011).

The mineralized zone is 2000 m long and 500–800 m wide. The concealed orebodies are located at depths >200 m, 125–650 m long, 1–6 m thick with a maximum thickness of 23.22 m, and yield total resources of 0.6 Mt of combined Cu, Pb, and Zn metal at average grades of 1.29% Cu, 1.69% Pb, 3.35% Zn, and 3.42 g/t Au (Jiang Qisheng et al., 2008). The mineralization is zoned from the base of the deposit upwards from lowermost Cu–(Au) orebodies (depths below –300 m) through Cu–Pb–Zn–(Au–Ag) orebodies (–300 to –200 m) to the uppermost Pb–Zn–(Ag) orebodies (–200 to –30 m; Jiang Qisheng et al., 2008).

The vein-type mineralization in the deposit has lens or vein shape and is hosted in xenoliths of Permian Qixia Formation limestones within the Yaojianling granodiorite porphyry stock (Fig. 7b). The ore types are characteristic by Cu–Au–(Ag) bearing lead–zinc, Cu-bearing pyrite, and Cu-bearing sphalerite ores (Jiang Qisheng et al., 2008; Liu Shaofeng, 2012). All of them are generally massive, and sulfides are generally present as veins within interlayer fractures of marbles, or occur as hypidiomorphic–xenomorphic granules and filling in the marble or marble-altered limestone units (Fig. 8a–d). Ore minerals mainly include pyrite, sphalerite, chalcopyrite, and galena, with minor amounts of bornite and chalcocite, etc. Gangue

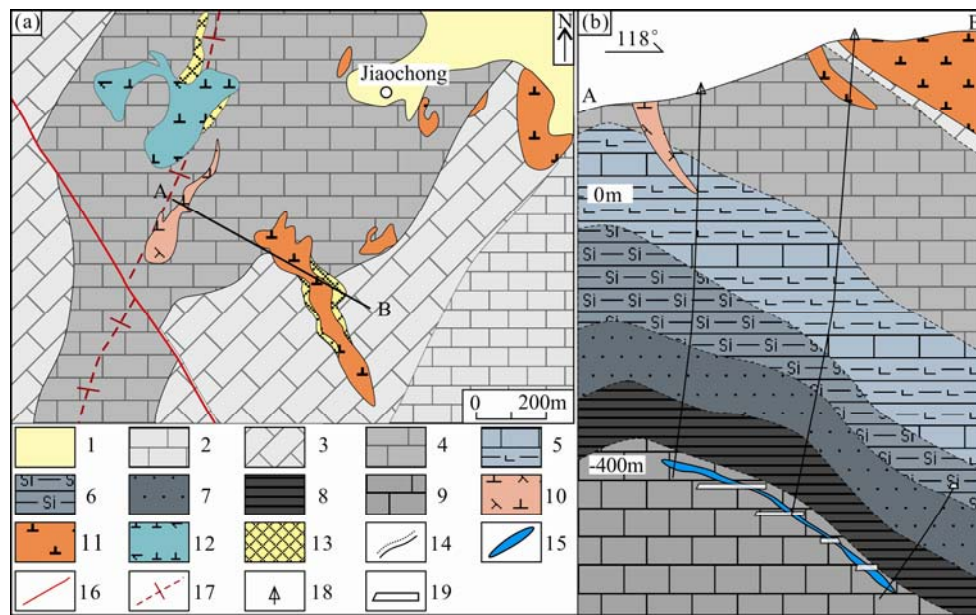


Fig. 5. Geological sketch map of the Jiaochong polymetallic deposit (a) and cross-section of the main orebody (b) (modified from Zhang Shoucheng and Zhao Yan, 2016).

1, Quaternary; 2, Middle Triassic Dongmaanshan Formation; 3, Lower Triassic Nanlinghu Formation; 4, Lower Triassic Helongshan Formation; 5, Lower Permian Yinkeng Formation; 6, Upper Permian Dalong Formation; 7, Upper Permian Longtan Formation; 8, Lower Permian Gufeng Formation; 9, Lower Permian Qixia Formation; 10, dioritic porphyrite; 11, diorite; 12, pyroxene diorite; 13, skarn; 14, observed/inferred geological boundary; 15, orebody; 16, faults; 17, anticline; 18, drill holes; 19, adits.

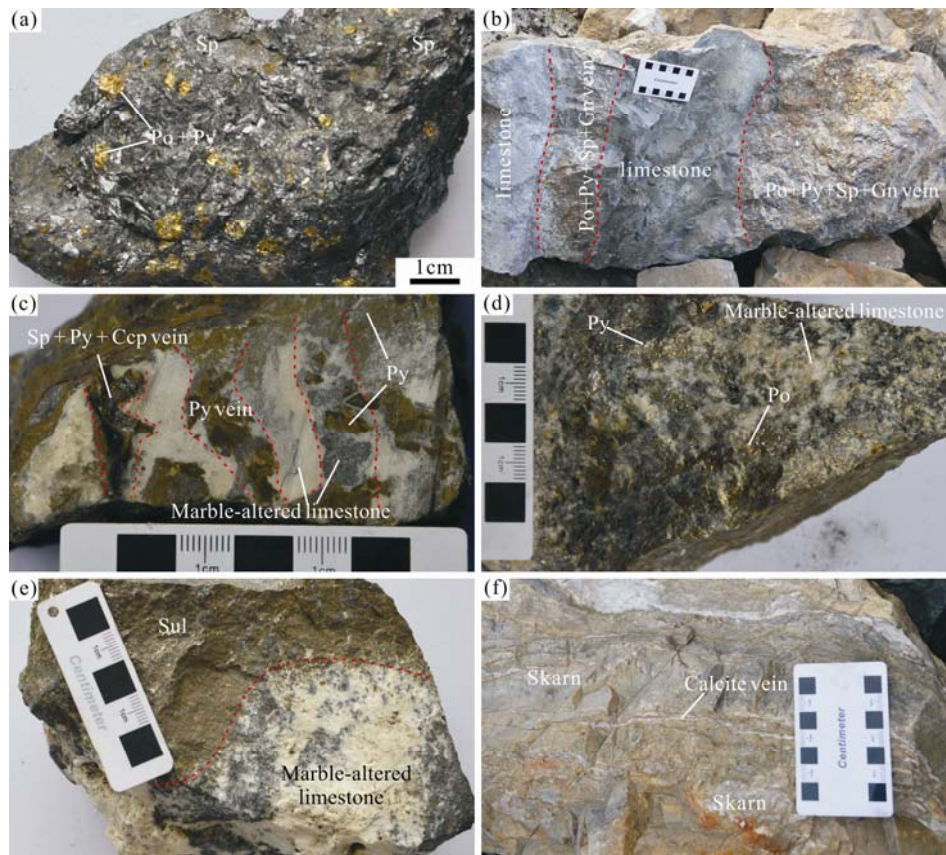


Fig. 6. Photographs showing alteration and mineralization characteristics of the Jiaochong deposit. (a) massive sphalerite ore with taxitic pyrite and pyrrhotite; (b) vein-type sulfide ore within limestone; (c) vein-hosted pyrite, sphalerite and chalcopyrite filling in marble or marble-altered limestones interlayer fractures; (d) pyrrhotite and pyrite occur as disseminations within marble-altered limestones; (e) sharp contrast between sulfide ore and marble-altered limestones; (f) ore-barrier skarn.

minerals are represented by calcite and quartz, with small amounts of barite and dolomite. The hydrothermal alteration associated with this mineralization is fairly simple and is divided into silicification and carbonate, pyrite, and weak barite alteration.

3.2.3 Hehuashan Pb-Zn deposit

The Hehuashan deposit is a newly discovered Pb-Zn deposit with great industrial significance (Liu Guangxian et al., 2017). It lies about 6 km northeast of the Jiaochong deposit (Fig. 1). The area around the deposit develops NW–SE, NE–SW and NNW–SSE trending faults that controlled the spatial distribution of the orebodies, as well as the mineralization-associated Hehuashan dioritic porphyrite apophyse (Liu Xiaoming, 2016). And about 42 orebodies have been discovered since 2010, but only two of these are significant sizes (No. 1 and No. 19 orebodies), with these orebodies containing 0.13 Mt Pb metal at a grade of 1.641%, 0.28Mt Zn metal at a grade of 1.937%, 112t Ag metal at a grade of 210.49 g/t, and 49kg Au metal at a grade of 7.50g/t (Liu Xiaoming, 2016). The main orebodies are generally stratiform or vein-shaped and hosted in limestone breccia of the Nanlinghu and Helongshan Formations. The location of mineralization directly controlled by faults and fracture zones (Fig. 9). The ores are divided into Pb–Zn, Zn, Pb, Pb–Zn–Ag, Pb–Ag, Zn–Ag, Ag and Au-bearing ore subtypes that are dominantly massive, vein-hosted, disseminated, and brecciated forms. Ore minerals contain galena, sphalerite, with lesser amounts of pyrite, limonite, marcasite, and minor amounts of native silver, native gold, arsenopyrite and chalcopyrite. Gangue minerals are mainly quartz and calcite, with lesser amounts of dolomite, barite and fluorite. The wall rocks alteration is extensive but weak intensity, mainly including extensive marmorization within Carboniferous to Triassic carbonates, as well as silicification and carbonate, pyrite, barite, fluorite, gypsum and chlorite alteration, with skarn only locally developed close to the Hehuashan intrusion.

Overall, the style of mineralization and alteration within the Hehuashan deposit above are similar to those present within the Jiaochong and Yaojialing deposits, indicating the genesis of the Hehuashan deposit falls into vein-type.

3.2.4 Baocun Au deposit

The Baocun Au deposit is located in the northeast end of the Shizishan orefield (Fig. 2a). It was thought to be a skarn-type deposit previously (Hu Huan et al., 2001; Ren Yunsheng et al., 2006). In recent years, however, Xiaochun et al. (2014) suggested that the Baocun deposit was mainly formed by skarn-type mineralization and also enriched by late-stage superimposed vein-type mineralization.

The rocks outcropped in the vicinity of the deposit are mainly Banded limestones of the Lower Triassic Helongshan and Nanlinghu Formations, as well as Baocun quartz diorite stock. The main ore-controlling structure is a nearly NS-trending fracture zone, which controlled the contact zone between quartz diorite intrusion and its corresponding wall rock as well as orebodies. The skarn-type orebody is lentoid and situated in contact zones

between intrusive and country rocks. Skarn mineral assemblages and corresponding hydrothermal alteration zone are well developed. The ore types are represented by Au (Cu)-bearing skarn ores. The vein-type orebody, by contrast, is generally vein-shaped and hosted in fault fracture zone, which is strictly controlled by fault or fracture, and superposed upon the skarn-type mineralization (Xu Xiaochun et al., 2014). The ores of the vein-type mineralization can be divided into Au-bearing breccia, massive Au-bearing pyrite and Au (Bi)-bearing quartz vein types. The hydrothermal alteration associated with this mineralization is divided into silicification, pyritization and kaolinization. All of geologic feature show that the Baocun Au deposit has compound characteristics of skarn- and vein-type.

4 Discussion

4.1 Unique identification of three mineralization types

As previously stated, in the Tongling ore district, polymetallic copper–gold mineralization can be divided into three subtypes according to the ore-controlling structure, host rock, mineral assemblage and hydrothermal alteration characteristics.

The skarn-type mineralization is the most economically significant type in this area. Such deposits mainly show skarnification, chloritization, epidotization and carbonation. Sometimes serpentinization and anhydritization are also common. The orebodies are mainly vein-like, lens-like and net-like, and are located near the contact zones between intrusive rock and carbonate wall rock. Some parts of stratiform orebodies are hosted in sedimentary rock as well. The ores typically display compact texture and massive, laminated or wriggly structures. The predominant ores are pyrrhotite, pyrite, chalcopyrite and magnetite; the minor ores include molybdenite, sphalerite and galena. The gangue minerals in the ores include mainly garnet, diopside and tremolite, but commonly also have small amounts of quartz, chlorite, epidote, and calcite. Locally, they have some serpentine, talc, humite, phlogopite, and anhydrite.

The porphyry-type mineralization is mainly hosted by intrusive bodies. The intrusive rock usually forms with a fine-grained or porphyritic texture, with intensive potassic, quartz-sericitic, and prophyllitic alteration. The ores are represented by a veined or veinlet-disseminated texture. Pyrite, pyrrhotite, magnetite and chalcopyrite are the main ore minerals, and quartz, K-feldspar, chlorite, epidote, and calcite are their gangue minerals.

The vein-type mineralization has its own characteristics that distinguish it from the previous two. This mineralization is only found in gold, silver–gold and lead–zinc deposits in this area. The orebodies mainly form as stratiform, lens or vein shapes, and are either hosted by country rock (mainly limestones or marbles) distal to intrusions, or within fractured zones that developed in intrusions and their limestone xenoliths. The vast majority of such ores form as veins and are strictly controlled by faults or fractures along host rock. The mineral compositions of the ores are commonly complex and mainly of metal sulfides, such as pyrrhotite, pyrite,

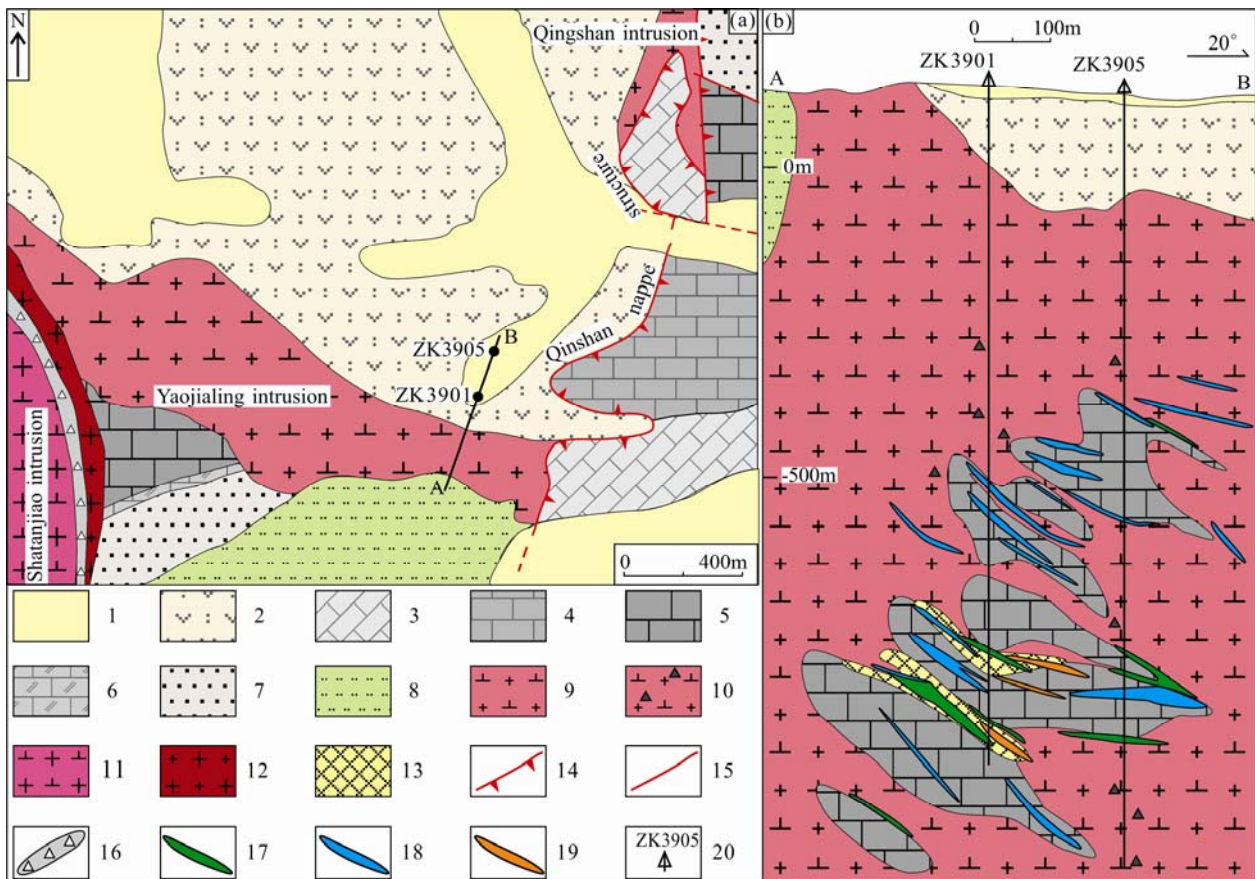


Fig. 7. Geological sketch map of the Yaojialing polymetallic deposit (a) and cross-section of No. 39 line of the main orebody (b) (modified from Zhong Guoxiong et al., 2014).

1, Quaternary; 2, Cretaceous Kedoushan Formation; 3, Lower Triassic Nanlinghu Formation; 4, Lower Triassic Helongshan Formation; 5, Lower Permian Qixia Formation; 6, Carboniferous Huanglong–Chuanshan Formation; 7, Upper Devonian Wutong Formation; 8, Middle–Lower Silurian Maoshan Formation; 9, granodiorite porphyry; 10, breccial granodiorite porphyry; 11, granodiorite; 12, granite porphyry; 13, skarn; 14, thrust faults; 15, faults; 16, crush zone; 17, Cu orebodies; 18, Pb–Zn orebodies; 19, Au orebodies; 20, drill holes and number.

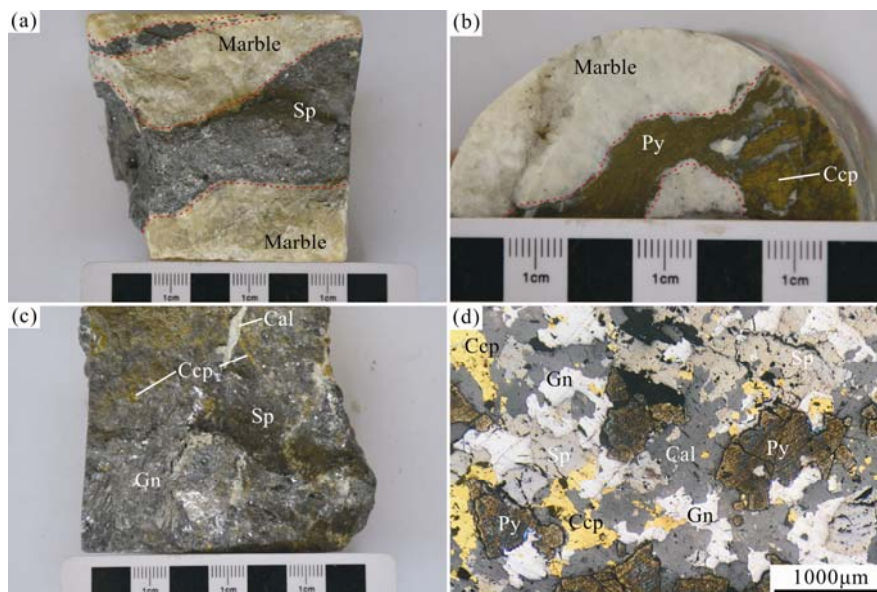


Fig. 8. Photographs showing representative ore types of the Yaojialing deposit.

(a) vein-hosted sphalerite filling in marble; (b) vein-hosted pyrite and chalcopyrite within marble; (c) massive sulfide ore consist of galena and sphalerite with minor chalcopyrite and is cut across by later calcite vein; (d) hypidiomorphic granular pyrite and xenomorphic sphalerite, galena and chalcopyrite filling in the marble (reflected light).



Fig. 9. Cross-section of No. 16 line of the main orebody in the Hehuashan deposit (modified from Liu Guangxian et al., 2017).

1, Lower Triassic Nanlinghu Formation; 2, Limestone breccia; 3, Thin-bedded limestone; 4, Dioritic porphyrite; 5, Orebodies; 6, Drill holes.

sphalerite and galena, etc., but also include gangue minerals such as calcite and quartz. The ore-bearing strata of the vein type deposit may be similar to those of stratabound skarn-type deposit, but the latter is closely related to skarnization and one end of this orebody is connected to intrusions (Xu Xiaochun et al., 2014). In contrast, the vein-type deposit is poorly associated with skarnization. This is exemplified by the fact that neither contact nor skarn zones contain orebodies. Moreover, the ore-forming temperature of a vein-type deposit is significantly lower than that of a stratabound skarn-type deposit (Table 1).

4.2 Spatial and temporal relationships between orebodies and intrusions in the Tongling ore district

4.2.1 Spatial associations between orebodies and intrusions

The Tongling ore district is well-known for stratabound, contact, interlayer, fissure, and crypto-explosive skarn mineralization (Chang Yinuo et al., 1991), although the porphyry- and vein-type mineralization in this area remains relatively understudied. These different types of deposits have different characteristics as outlined above. The polymetallic copper–gold orebodies have spatially close genetic relationships with small-medium

intermediate-acid intrusions formed by Yanshanian magmatism. They are commonly located along the contact zones between intrusions and their country rock. When intrusions emplaced into dolomite, dolomitic limestone or limestone, it is normal that skarn-type mineralization develops, and it shows well-defined skarn alteration zoning from the intrusion center outward. Some stratabound skarn-type orebodies are located within sedimentary rock distal to intrusions, as is the case for the upper part of the Dongguashan deposit. Generally, however, these orebodies occur within contact aureoles in close relation to skarnization, and one end of these orebodies is connected to an intrusion (Fig. 2b). The same situation occurs in the Xinqiao Cu–Au–S deposit, which is also a typical stratabound skarn-type deposit (Chang Yinuo and Liu Xuegui, 1983). This indicates that magmatic hydrothermal activity played a dominant part in ore-forming. The porphyry-type mineralization is generally located in areas where intermediate–acid intrusions entered sedimentary detrital rock or silicalites. These deposits connected with skarn mineralization in the same area to form a porphyry–skarn system (e.g., the Dongguashan Cu–Au and Hucunshan Cu–Mo–(Au) deposits). The vein-type mineralization usually occurred in country rocks distal to intrusions (e.g., the Jiaochong and Hehuashan polymetallic deposit), or within fracture zones that developed in intrusions. It sometimes overprints earlier skarn- or porphyry-type mineralization (as is the case for the Yaojialing polymetallic deposit and Baocun Au deposit; Chu Guozheng, 2003; Liu Shaofeng, 2012; Xu Xiaochun et al., 2014). The spatial distribution of mineralization within the Tongling ore district is also associated with the relative depth of the intermediate–acid intrusion. The vein-type deposits are generally located in shallow locations where country rock is relatively distal to intrusions. Skarn-type deposits are located at moderate depths and connected with sedimentary carbonate country rock of intrusions. Porphyry-type deposits are found in relatively deeper locations where intrusions enter sedimentary detrital rock or silicalites, constituting a space distribution pattern of a trinity or multi-positional pattern (Li Wenda, 1989; Chang Yinuo et al., 1991; Zhai Yusheng et al., 1992).

4.2.2 Timing of diagenesis and mineralization

The Tongling ore district contains abundant Yanshanian intrusions clustered within the Tongguanshan, Shizishan, Xinqiao, Fenghuangshan, and Shatanjiao areas (Fig. 1; Xing Fengming et al., 1996; Pan and Dong, 1999; Xie et al., 2009; Wang et al., 2010; Deng et al., 2011; Xu Xiaochun et al., 2012; Wu Cailai et al., 2013). The main lithologies are pyroxene diorite, quartz diorite and granodiorite, and these are generally present as small stocks and dikes (Pan and Dong, 1999) that were emplaced at 135–147 Ma. Previous research suggests that all of the polymetallic copper–gold deposits in the Tongling ore district are temporally related to this Yanshanian magmatism, with mineralization occurring at 135–145 Ma. This suggests that the mineralization is genetically linked to the magmatic–hydrothermal fluids associated with the Yanshanian intrusions (Table 2).

Table 2 Summarized geochronological data for typical copper-gold polymetallic deposits and related magmatic rocks in the Tongling ore district

Deposit	Deposit type	Rock-forming age			Ore-forming age			Ref.
		Host rock	Dating method	Age (Ma)	Ore type	Dating method	Age (Ma)	
Hucunnan	porphyry–skarn	granodiorite		140.0±2.6	Mo-bearing ore	molybdenite Re-Os	140.4±1.9	1, 2
Dongguashan		quartz diorite		135.5±2.2	Cu-bearing sulfide quartz	molybdenite Re-Os	139.1±1.6	2, 3, 4
Chaoshan	skarn	pyroxene diorite	zircon U-Pb (SHRIMP)	139.1±2.3	Cu-bearing serpentine	zircon U-Pb (LA-ICP MS)	318.3±2.6	2, 5, 6
Tongguanshan	skarn	quartz diorite			141.8±1.0	Au-bearing magnetite ore	quartz inclusion Rb-Sr	
Laomiaojishan	skarn				Au-bearing pyrrhotite	pyrrhotite Re-Os	141.7±9.9	7, 8
Yaoyuanshan	skarn	granodiorite		141.0±1.1	skarn ore	flogopite Ar-Ar	135.5±0.5	
Datuanshan	skarn	quartz diorite		139.3±1.2	skarn ore	flogopite Ar-Ar	144.9±0.4	9
Laoyaling	skarn				Mo-bearing skarn	molybdenite Re-Os	141.1±1.4	10, 11
Jinkouling	skarn	granodiorite	biotite Ar-Ar	137.3±1.4	Mo-bearing ore	molybdenite Re-Os	139.1±2.7	12
							Mo-bearing ore	molybdenite Re-Os
					Mo-bearing black shale	whole rock Re-Os	234.2±7.3	13
					skarn ore	molybdenite Re-Os	137.0±2.0	7, 14
					sulfide quartz stockwork	pyrite Re-Os	319±13	15
Xinqiao	skarn	quartz diorite		139.6±1.5		quartz inclusion Rb-Sr	138.0±2.3	16
					sulfide ore	pyrite Re-Os	138±26	17
						pyrite Re-Os	393±40	17
Shujiadian	skarn	pyroxene diorite		139.2±2.1	Mo-bearing ore	molybdenite Re-Os	140.6±2.0	18
Shatanjiao	skarn	granodiorite		144.1±1.5	Mo-bearing ore	molybdenite Re-Os	141.8±1.6	10, 19
Yaojialing	Porphyry–skarn–vein	granodiorite	zircon U-Pb (LA-ICP MS)	141.4±1.7	Mo-bearing ore	molybdenite Re-Os	142.5±1.6	20, 21
Baocun	skarn–vein	quartz diorite						
Jiaochong	vein	pyroxene diorite		128.5±2.1				22
		dioritic porphyrite		128.0±2.2				23
		dioritic porphyrite		133.0±2.1				24
Hehuashan	vein	quartz diorite		130.1±1.7				24
Jiguanshi	vein	quartz diorite		136.1±3.0				25

Note: 1, this paper; 2, Xu Xiaochun et al. (2008); 3, Lu Sanming (2007); 4, Guo Weimin (2010); 5, Chu Guozheng (2003); 6, Wang et al. (2008); 7, Meng Yifeng et al. (2004); 8, Wu Cailai et al. (2010); 9, Qu et al. (2012); 10, Mao Jingwen et al. (2004); 11, Wu Cailai et al. (2008); 12, Xie Zhi et al. (2002); 13, Yang Gang et al. (2004); 14, Zhou Taixi et al. (1988); 15, Guo Weimin et al. (2011); 16, Zhang et al. (2017); 17, Wang Yangyang et al. (2015); 18, Wang Shiwei et al. (2012); 19, Wu Cailai et al. (2013); 20, Zhong Guoxiong et al. (2014); 21, Yin Yanduan et al. (2016); 22, Xu Xiaochun et al. (2018a, b); 23, Que Chaoyang et al. (2013); 24, Liu Guangxian et al. (2017); 25, Xie et al. (2009)

Emerging research has suggested that a small number of the intrusions in the study area were formed at 133–124 Ma (Xu Xiaochun et al., 2018a, b; Table 2). This indicates that there is still later magmatism and that correlative mineralization took place in the study area. However, some research also yielded Hercynian isotopic ages for mineralization in this area (Table 2; Yang Gang et al., 2004; Guo Weimin, 2010; Guo Weimin et al., 2011; Wang Yangyang et al., 2015), and in this work, the role of the Late Paleozoic submarine exhalative processes was emphasized and suggested that this district also contained Hercynian mineralization. However, these isotopic ages are suspect due to the discrete acquisition of data and the immaturity of the relational analysis methods used. Some geological evidence is usually isolated, while microcosmic geochemical records of the earlier Late Paleozoic mineralization have proven to be less contributive or mostly overprinted by Yanshanian hydrothermal mineralization (Xu Xiaochun et al., 2010; Zhou Taofa et al., 2016). There is no compelling evidence for Late Paleozoic syngenetic hydrothermal activity, and this hypothesis requires more geological facts at both the regional and deposit scale, as well as more support in geochemical data, to be confirmed.

4.3 Geochemical characteristics of the fluid inclusions and stable isotopes of the deposits

4.3.1 Geochemical characteristics of fluid inclusions

Fluid inclusions of transparent minerals (quartz, garnet, and calcite) from deposits in the study area are divided roughly into three types: vapor-rich, liquid-rich, and daughter-crystal-bearing multiphase inclusions. Inclusions from individual deposits homogenize over a wide range of temperatures (Xu Xiaochun et al., 2014), with these temperatures decreasing from the earlier to the later stages of mineralization. For example, fluid inclusions from the Dongguashan Cu–Au deposit homogenize at temperatures of 568–411°C, 440–173°C, and 286–110°C for the early silicate (skarn) stage, middle quartz-sulfide stage, and late carbonate stage of the mineralization, respectively (Lu Sanming, 2007). Fluid inclusion salinities also behave similarly, where earlier stages of mineralization are associated with high salinity fluids and later stages of mineralization are associated with lower salinity fluids. These inclusions also contain gases those of which H₂O and CO₂ are predominant with lesser amounts of CH₄ and N₂. The liquid components of these inclusions are mostly F⁻, Cl⁻, and SO₄²⁻ anions and K⁺, Na⁺, Ca²⁺, and Mg²⁺ cations (Lou Jinwei, 2012; Xu Xiaochun et al., 2014). The

conditions of the hydrothermal fluids represented by these inclusions are high temperature and high salinity, CO_2^- , F^- , and Cl^- -rich fluids. This indicates that these hydrothermal fluids were derived from magma.

4.3.2 Isotope geochemistry

The stable isotopic compositions of the deposits and associated geological units provide evidence of fluids sourcing. Here we focus on the isotope geochemistry on the basis of several representative porphyry-, skarn-, and vein-type deposits in the study area to discuss the sources of ore-forming fluids and metals.

The $\delta^{34}\text{S}$ values of sulfide samples from representative porphyry, skarn and vein-type orebodies have been summarized in Table 3 and Fig. 10. These $\delta^{34}\text{S}$ values display a considerable range of variation between -5.3‰ and $+10.2\text{‰}$, but cluster between 0‰ and $+7.0\text{‰}$ (Fig. 10). This corresponds closely to the whole-rock sulfur isotopic composition of Yanshanian intrusions (-2.2‰ to $+7.0\text{‰}$; Li Wenda et al., 1998; Liu Zhongfa et al., 2014; Xu Xiaochun et al., 2014), but is distinct from the $\delta^{34}\text{S}$ values of sedimentary rock from the Tongling ore district (-35.4‰ to -4.6‰ ; Liu Yuqing et al., 1984; Zhou Zhen, 1984; Tang Yongcheng et al., 1998; Liu Zhongfa et al., 2014). Moreover, the $\delta^{34}\text{S}$ values of sulfides from these three types of deposits exhibit a bell shape distribution and a similar range in Fig. 10. This suggests that the sulfur in these deposits was derived from the same source, most likely Yanshanian granitic magma.

Common Pb isotopic compositions of the three types of deposits as well as sedimentary and magmatic rock are presented using $^{206}\text{Pb}/^{204}\text{Pb}$ vs. $^{207}\text{Pb}/^{204}\text{Pb}$ and $^{206}\text{Pb}/^{204}\text{Pb}$ vs. $^{208}\text{Pb}/^{204}\text{Pb}$ diagrams (Fig. 11). With the exception of a few outliers, the Pb isotopic compositions of pyrite, pyrrhotite, chalcopyrite and galena are basically consistent and the data dots generally fall within the field of magmatic Pb. However some did fall in the overlapping area between magmatic Pb and sedimentary Pb (Fig. 11). This indicates that the Pb and other metallic elements within these deposits were also derived from magma or from magmatic rock. Although it is not possible to completely exclude sediments as the source of metals, it is certainly the case that any sediment-derived Pb is secondary compared to the contribution of magmatic Pb.

Some data on hydrogen and oxygen isotopes in different stages of mineralization from all three types of deposits were collected and are shown in Fig. 12 and Table 4. All the data again are indicative of a magmatic source. This is supported by: (1) the data points of H–O isotope are mainly plotted in the magmatic water area and its transition region to the meteoric water area (Fig. 12). No genetic connection has been shown with sea water. (2) The H–O isotopic compositions from early silicate or skarn stage are mainly located in magmatic water and its vicinity (Fig. 12). This suggests that ore-forming hydrothermal fluids are intimately related to regional magmatism. (3) The $\delta^{18}\text{O}_{\text{H}_2\text{O}}$ fluid values for the deposits range from -2.7‰ to $+11.7\text{‰}$ (Table 4) and decrease in value with the evolution of the fluids (Fig. 12; from the skarn or silicate stage to quartz-sulfide stage, then to the quartz-carbonate stage). This suggests that the ore-forming fluids

Table 3 Sulfur isotope compositions of sulfides from the polymetallic copper-gold deposits in the Tongling ore district

mineralization	locality	sample	$\delta^{34}\text{S}_{\text{CDT}}$ (‰)	Mean value	Data sources
Porphyry-type	Deeper Hucunshan	Pyrite	2.0–3.3	2.7 (n=2)	This paper
		Chalcopyrite	2.2–2.3	2.3 (n=2)	
		Molybdenite	2.6–4.0	3.5 (n=4)	
		Sphalerite	4.5	4.5 (n=1)	
	Deeper Dongguashan	Pyrite	4.1–5.7	5.0 (n=5)	Liu Zhongfa et al., 2014; Xu Zhaowen et al., 2007
		Pyrite	3.6–6.0	4.9 (n=8)	Wang et al., 2014
	Pyrrhotite	5.1–5.7	5.4 (n=3)		
	Chalcopyrite	4.3–5.1	4.7 (n=4)		
	Shujiadian	Molybdenite	6.5–6.7	6.6 (n=2)	Liu Shaofeng, 2012
		Pyrite	-2.6–0.8	-1.5 (n=3)	
	Yaojialing	Pyrite	0.4–2.8	1.8 (n=10)	Yue Zilong, 2015
	Guihuachong	Pyrite	0.1–0.7	0.4 (n=3)	Xu Zhaowen et al., 2007; Xu Xiaochun et al., 2010; Liu Zhongfa et al., 2014 Yang Heming, 2016 Wang Jianzhong et al., 2008 Tian Shihong et al., 2005 Zhang et al., 2017 Liu Shaofeng, 2012 Qu Hongying, 2010 Liu Shaofeng, 2012 Zhang Zhihui et al., 2013 Yang Qirong et al., 2010
Chalcopyrite		3.0–10.2	5.1 (n=23)		
Upper Dongguashan	Pyrrhotite	4.8–5.7	5.3 (n=5)		
	Chalcopyrite	4.3–5.3	4.8 (n=2)		
	Sphalerite	5.3	5.3 (n=1)		
Upper Hucunshan	Pyrite	1.9	1.9 (n=1)		
	Chalcopyrite	2.4–3.6	2.8 (n=3)		
Skarn-type	Chaoshan	Pyrite	6.2–7.8	7.1 (n=3)	
		Pyrrhotite	6.4–9.3	7.6 (n=3)	
	Sphalerite	8.7	8.7 (n=1)		
	Galena	6.2–6.3	6.3 (n=2)		
Xiaotong- guanshan	Pyrite	3.6–6.0	5.0 (n=5)		
	Chalcopyrite	4.2–4.5	4.3 (n=3)		
Xinqiao	Pyrite	0.5–4.5	2.9 (n=24)		
	Pyrrhotite	4.4	4.4 (n=1)		
	Sphalerite	2.6	2.6 (n=1)		
Yaojialing	Galena	1.3–1.7	1.5 (n=2)		
	Pyrite	-1.1–0.7	-0.9 (n=2)		
Fenghuangshan	Chalcopyrite	-1.3–0.2	-0.8 (n=2)		
	Pyrite	-5.1–5.2	2.3 (n=17)		
Vein-type	Yaojialing	Pyrite	0.3–0.9	0.6 (n=3)	
		Sphalerite	-0.2–1.3	0.5 (n=3)	
	Jiaochong	Pyrite	2.1–5.0	4.0 (n=7)	
		Pyrrhotite	3.6–4.4	4.0 (n=4)	
Tianmashan	Sphalerite	3.9–4.7	4.3 (n=3)		
	Galena	2.1–3.2	2.7 (n=3)		
	Pyrite	5.4–8.0	6.9 (n=8)		

in the earlier stage were dominated by magmatic fluids with minor amounts of meteoric water, whereas the later stage fluids were magmatic but mixed with large amounts of meteoric water.

The $\delta^{13}\text{C}$ and $\delta^{18}\text{O}$ values of calcite, dolomite, quartz and siderite from the major deposits in the Tongling ore district also vary significantly ($\delta^{13}\text{C}$ values from -8.7‰ to $+5.0\text{‰}$; $\delta^{18}\text{O}$ values from $+6.7\text{‰}$ to $+18.7\text{‰}$) but cluster between -7.0‰ to $+2.0\text{‰}$ and $+9.0\text{‰}$ to $+16.0\text{‰}$ (Fig. 13), respectively. Most of the samples were from in or near the granite area, but were obviously affected by carbonate dissolution. The values above are similar to the C–O isotopic compositions of magmatic–hydrothermal fluids ($\delta^{13}\text{C}$ values from -9‰ to -3‰ and $\delta^{18}\text{O}$ values from $+6\text{‰}$ to $+13\text{‰}$; Taylor and Forester, 1979; Ishihara, 1981; McCulloch and Chappell, 1982; Taylor, 1986), but significantly different from the values of normal

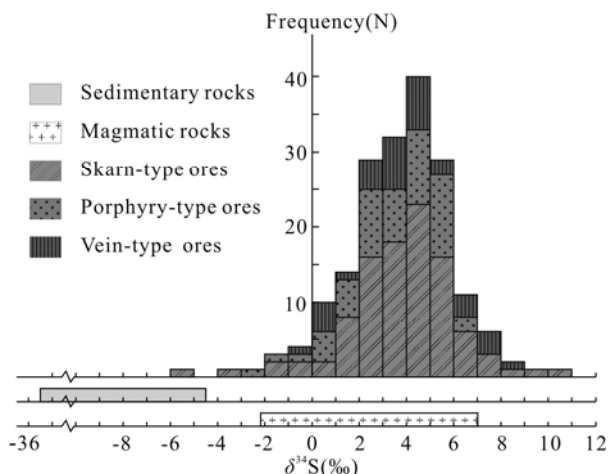


Fig. 10. Histogram of the S isotope compositions of sulfides in skarn-, porphyry-, and vein-type deposits from the Tongling ore district. Also shown is the range of S isotope compositions of the related sedimentary and magmatic rocks. Data from Table 3.

sedimentary carbonates ($\delta^{13}\text{C}$ values from +2.2‰ to +5.9‰ and $\delta^{18}\text{O}$ values from +23‰ to +24.5‰). This suggests that the carbon in the deposits may also have a magmatic source, with only minor amounts derived from sediments in this region.

Overall, the ore-forming fluids as well as the metal elements and related chemical elements that generated the porphyry-, skarn-, and vein-type deposits in the study area are derived from Yanshanian granitic magma. These magmatic fluids mixed with significant amounts of meteoric fluids during the later stages of mineralization.

4.4 Metallogenic model for mineralization within the Tongling ore district

The spatial and temporal coupling between the

polymetallic copper–gold deposits and the Yanshanian intrusions suggests a genetic link between mineralization and magmatism in the Tongling ore district. The fact that all the skarn-, porphyry-, and vein-type deposits have somewhat similar geochemical characteristics of fluid inclusions and stable isotopes suggests that they may have formed as part of a unified magmatic–hydrothermal system. Here, we outline a unified porphyry–skarn–vein model for the polymetallic copper–gold deposits that incorporates the geology of this area (Fig. 14), as well as the processes that formed the deposits. Compared with previous genetic models suggested for this area (Li Wenda, 1989; Chang Yinfo et al., 1991; Tang Yongcheng et al., 1998; Pan and Dong, 1999; Mao Jingwen et al., 2009), our new model emphasizes the importance of skarn-type deposits in the Tongling ore district, but also demonstrates that this area is highly prospective for porphyry- and vein-type deposits. This emphasizes the importance of these two deposit types for future research and exploration in this area.

As an important part of the MLYB, the Tongling ore district is constrained by the unified geodynamic settings of eastern China. This metallogenic model holds that eastern China was undergoing tectonism associated with continental intraplate orogenesis between the Late Jurassic and Early Cretaceous (125–145 Ma; Xu Xiaochun et al., 2012). The early part of this period (135–145 Ma) recorded a change in stress fields from compressional to extensional as a result of the subduction of the paleo-Pacific Plate in the range 145–165±5 Ma. The thickened lithosphere, caused by the previous N–S oriented collision and convergence of the North China and Yangtze cratons and subsequent northwestward-directed subduction of the paleo-Pacific Plate, began to melt by decompression and generated basaltic magma. The basaltic magma underplated the lower crust and formed voluminous adakite-like magma as a result of crust–mantle interaction.

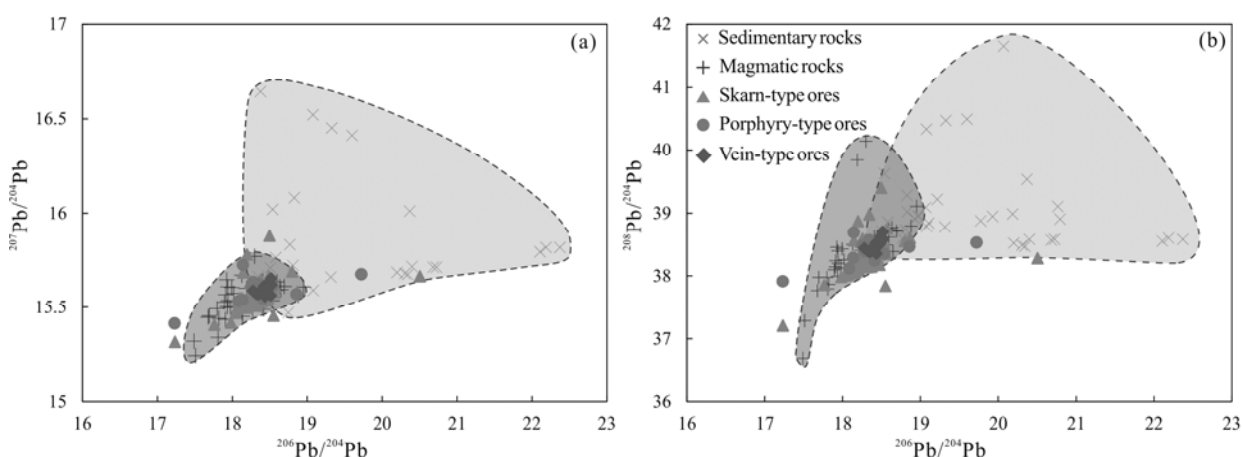


Fig. 11. (a) $^{206}\text{Pb}/^{204}\text{Pb}$ vs. $^{207}\text{Pb}/^{204}\text{Pb}$ and (b) $^{206}\text{Pb}/^{204}\text{Pb}$ vs. $^{208}\text{Pb}/^{204}\text{Pb}$ diagrams showing the Pb isotope compositions of the polymetallic copper–gold deposits in the Tongling ore district.

Data sources: the Pb isotopic compositions of magmatic and sedimentary rocks from the Tongling ore district are cited from Zhou Zhen (1984); Huang Bin (1991); Zhai Yusheng et al. (1992); Chu Guozheng (2003); Li Jinwen (2004); Yu Gang (2004); Lu Sanming (2007); Zang Wenshuan et al. (2007); Xie Jiancheng (2008). The Pb isotopic compositions of vein-type ores are represented by the Jiaochong (Zhang Zhihui et al., 2013) and Yaojialing deposits (Liu Shaofeng, 2012). Porphyry-type ores are from the Hucunna (this paper) and Dongguashan deposits (Liu Zhongfa et al., 2014). Skarn-type ores are cited from Dongguashan (Xu Zhaowen et al., 2007; Liu Zhongfa et al., 2014); Hucunna (Chu Guozheng, 2003); Chaoshan, Baocun, Xiaotongguan-shan (Li Jinwen, 2004); Xingqiao (Zang Wenshuan et al., 2007; Zhang et al., 2017); Fenghuangshan deposits (Shao Yongjun et al., 2007).

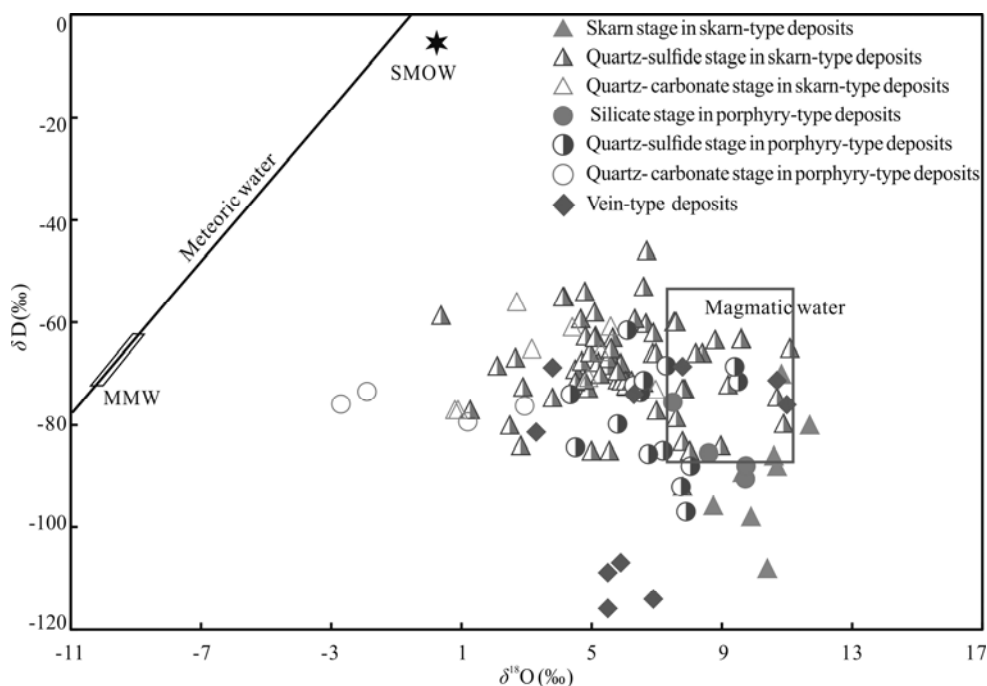


Fig. 12. $\delta^{18}\text{O}$ (‰) vs. δD (‰) diagrams of ore-forming hydrothermal fluids for the three types of mineralization. Data from Table 4.

MME-the Mesozoic meteoric water; SMOW-standard mean ocean water.

Table 4 Hydrogen and oxygen isotope compositions of fluid inclusions in minerals from the Tongling ore district

Mineralization	Locality	Description	Sample	$\delta^{18}\text{O}_{(\text{H}_2\text{O})}$ (‰)	Mean value	$\delta^{18}\text{D}_{(\text{H}_2\text{O})}$ (‰)	mean value	Data sources	
Porphyry-type	Deeper Hucunshan	Silicate stage	Quartz	7.5–8.6	8.1 (n=2)	-85.5–75.5	-80.5 (n=2)	This paper	
		Quartz-sulfide stage	Quartz	5.8–9.5	7.2 (n=8)	-79.8–61.6	-70.9 (n=8)		
		Quartz-carbonate stage	Calcite	-2.7–1.2	-0.8 (n=2)	-79.4–75.9	-77.7 (n=2)		
	Guihuangchong	Quartz-sulfide stage	Quartz	4.4–7.9	6.5 (n=3)	-97–74	-85.3 (n=3)	Wang Shiwei, 2015	
		Silicate stage	Quartz	9.7	9.7 (n=2)	-90.5–88.0	-89.2 (n=2)	Zuo Xiaomin et al., 2016	
		Quartz-sulfide stage	Quartz	4.5–8.0	6.8 (n=4)	-92.0–84.3	-87.5 (n=4)		
Skarn-type	Upper Dongguashan	Quartz-carbonate stage	Calcite	-1.9–3.0	0.5 (n=2)	-76.3–73.4	-74.8 (n=2)	Xu Zhaowen et al., 2005; Lu Sanming, 2007; Lu Jianjun et al., 2008; Liu Zhongfa et al., 2014	
		Skarn stage	Quartz	9.6–11.7	10.7 (n=2)	-80–63.1	-71.6 (n=2)		
		Quartz-sulfide stage	Quartz	3.8–11.1	6.4 (n=37)	-84.0–55.0	-67.4 (n=37)		
	Tongguanshan	Quartz-carbonate stage	Calcite	3.2–7.0	5.1 (n=6)	-73.0–60.8	-66.0 (n=6)	Tian Shihong et al., 2004	
		Upper Hucunshan	Quartz-sulfide stage	Quartz	7	7 (n=1)	-77.1		-77.1 (n=1)
		Skarn stage	Garnet	9.9–10.7	10.4 (n=4)	-108.0–86.0	-95.0 (n=4)		
Fenghuangshan	Chaoshan	Quartz-sulfide stage	Quartz	5.1–5.4	5.2 (n=2)	-63.0–58.0	-60.5 (n=2)	Tian Shihong et al., 2004	
		Quartz-carbonate stage	Calcite	0.8–4.8	2.3 (n=4)	-77.0–54.0	-66.0 (n=4)		
		Skarn stage	Garnet	10.8	10.8 (n=1)	-70.0	-70.0 (n=1)		
	Datuanshan	Quartz-sulfide stage	Quartz	1.3–8.0	4.7 (n=8)	-92.0–63.0	-80.9 (n=7)	Qu Hongying, 2010	
		Quartz-sulfide stage	Calcite	5.3–5.6	5.5 (n=3)	-85.0–65.0	-73.3 (n=3)		
		Quartz-sulfide stage	Quartz	5.6–8.6	6.9 (n=2)	-66.0–65.0	-65.5 (n=2)		
Vein-type	Xishizishan	Quartz-sulfide stage	Calcite	6.6–6.7	6.7 (n=2)	-53.0–46.0	-49.5 (n=2)	Tian Shihong et al., 2004	
		Skarn stage	Garnet	8.7	8.7 (n=1)	-95.8	-95.8 (n=1)		
		Quartz-sulfide stage	Quartz	2.1–6.6	4.6 (n=6)	-72.5–67.0	-69.8 (n=6)		
	Yaojialing	Skarn stage	Garnet	9.6	9.6 (n=1)	-89.2	-89.2 (n=1)	Li Jinwen, 2004; Lu Sanming, 2007	
		Quartz-sulfide stage	Quartz	4.9	4.9 (n=1)	-65.8	-65.8 (n=1)		
		Quartz-sulfide stage	Quartz	2.7	2.7 (n=1)	-66.9	-66.9 (n=1)		
Jiguanshi	Quartz-sulfide stage	Quartz	5.5	5.5 (n=1)	-85.5	-85.5 (n=1)	Zhan Changfan, 2013		
		Quartz	3.3–6.9	4.7 (n=3)	-114.1–68.8	-88.1 (n=3)			
		Calcite	5.5–5.9	5.6 (n=3)	-115.9–106.9	-110.6 (n=3)			
		Quartz	6.3–11.0	9.0 (n=4)	-76.0–68.6	-72.5 (n=4)	Lu Sanming, 2007		

The magma may have mixed and migrated along deep-seated E–W-trending faults before being emplaced to form the three types of intermediate–acid intrusive rock that is common in the Tongling ore district, namely pyroxene

diorites, quartz diorites, and granodiorites. The magma within deep magma chambers continued to evolve and eventually exsolved magmatic–hydrothermal fluids that migrated along the same deep-seated faults to interact with

shallow intrusive bodies and the country rock. These fluids also became enriched in metallic elements that eventually enabled the formation of the mineral deposits. These fluids might also have mixed with meteoric fluids that migrated downwards via the same faults, with the resulting fluids ascending as a result of heating by the underlying magma. These metal-enriched magmatic–hydrothermal fluids eventually migrated to the shallow intrusions and interacted with overlying sedimentary detrital rock or silicalites. They formed lentoid, veinlet-stockwork, and veinlet-disseminated mineralization within these granitoid intrusions and the country rock. This hydrothermal activity also generated alteration zones typical of porphyry-type systems and affected both the intrusions and the country rock. The activity formed porphyry-type deposits exemplified by the deeper Dongguashan porphyry Cu–Au deposit (Fig. 14). The continued ascent of the ore-forming hydrothermal fluids caused these fluids to enter the detachments between sandstones of the Upper Devonian Wutong Formation and dolomites or dolomitic limestones of the Upper Carboniferous Huanglong and Chuanshan Formations (Fig. 14). This further migration was associated with progressive water–rock interaction and metasomatism between hydrothermal fluids and magnesian carbonates. This generated stratiform mineralization characterized by wriggly and laminated ores associated with magnesian skarns and retrograde metamorphic mineral assemblages. Chang Yinfo et al. (1991) termed this style of mineralization stratabound skarn deposits. These deposits containing orebodies with locations controlled by fold axes and interlaminar slip structures, as exemplified by the Upper Dongguashan Cu–Au deposit. The further migration of hydrothermal fluids along the contact zones between the granitoid intrusions and surrounding carbonate country rock caused intense metasomatism of both the granitoids and the Late Carboniferous to Middle Triassic carbonate rock (Fig. 14). This resulted in thermal metamorphism and skarn-type hydrothermal alteration, as exemplified by the Hucunna Cu–Mo–(Au) deposit. In this study, the above two deposit subtypes are assigned to skarn-type deposits. The migration of hydrothermal fluids through country rock distal to intrusions, or through fracture zones developed in intrusions (Fig. 14) also generated vein- or lens-shaped mineralization. This occurred in the form of massive sulfide and vein-hosted quartz- or carbonate-sulfide ores associated with significant carbonate and pyrite alteration and the generation of moderate to low temperature metal sulfide assemblages. This style of mineralization is herein termed vein-type mineralization, as exemplified by the Jiaochong deposit.

As mentioned above, all three types of mineralization within the Tongling ore district are associated with a unified magmatic–hydrothermal system and are genetically related. This is supported by the fact that these mineralization styles often overprint each other, as exemplified by the presence of porphyry–skarn (e.g., the Dongguashan, Hucunna deposit), skarn–vein (e.g., the Baocun deposit), and porphyry–skarn–vein (e.g., the Yaojialing deposit) deposit types. The deposits have systematic spatial and temporal distributions, with deposit

formation occurring slightly after the related intermediate–acid intrusive activity, and with the polymetallic Au–(Cu, Ag) mineralization forming slightly after the Cu–(Mo, Au) mineralization within the Tongling ore district. The porphyry-type deposits in this ore district are generally located at depth, with skarn-type deposits located at moderate depths and vein-type deposits located at shallow depths. The mineralizing systems are also zoned, with porphyry-type deposits located within or proximal to intrusions, skarn-type deposits located within contact zones, and vein-type deposits generally distal to intrusions and hosted by country rock, with the exception of a few of these deposits that are hosted by limestone xenoliths within intrusions or within fracture sets in intrusions. This zoning extends to the ore-forming element associations in this ore district, which change from deep Cu–(Mo, Au) mineralization to shallow polymetallic Au–(Cu, Ag) mineralization and from proximal Mo mineralization through Cu and Au zones to distal Ag–Pb–Zn mineralization.

However, it should also be noted that the genesis of stratiform orebodies (e.g., the Upper Dongguashan and Xinqiao deposits) in the study area remains controversial, with models suggesting these deposits are derived from either Yanshanian magmatic–hydrothermal fluids (Pan and Dong, 1999; Xu and Zhou, 2001; Deng Jinfu et al., 2002; Mao Jingwen et al., 2004, 2009; Xu et al., 2011; Xu Xiaochun et al., 2010, 2014; Zhang et al., 2017) or formed as a result of Hercynian SEDEX type processes that were overprinted by later Yanshanian magmatism (Gu Lianxing and Xu Keqin, 1986; Tang Yongcheng et al., 1998; Yang Zhusen et al., 2004; Zeng Pusheng et al., 2004, 2005; Gu et al. 2007; Lu Jianjun et al., 2008; Guo Weimin et al., 2011; Hou Zengqian et al., 2011). The key question is whether the Hercynian sediments in the study area merely hosted the mineralization or actually supplied material to the deposits. Zeng Pusheng et al. (2004) and Yang Zhusen et al. (2004) reported that hydrothermal sedimentary rock is widely developed in this area, all of which is closely related to massive sulfide deposits. This has been used as evidence of the presence of Hercynian SEDEX systems, although the extent of this activity remains unclear and requires further research. Both the stratiform orebodies and the footwall stockwork mineralization occur in combination in the Xinqiao deposit, which is similar to the style of mineralization expected for SEDEX-type systems (Xu and Zhou 2001; Hou Zengqian et al., 2011). However, the mineral assemblage and alteration of the footwall stockwork mineralization in this area are entirely distinct from typical SEDEX deposits (Mao Jingwen et al., 2009; Mao et al., 2011; Zhang et al., 2017). Thus there is no direct evidence of the presence of Hercynian SEDEX mineralization in the Tongling ore district. In addition, the isotopic ages of the purported Hercynian mineralization vary considerably, again casting doubt on the timing of the formation of this mineralization (Table 2). This led some researchers to suggest that these Hercynian sediments merely acted as a preferential host for mineralization. The fact that the stratiform orebodies in this area are all located close to intrusive bodies also suggests the presence of a genetic

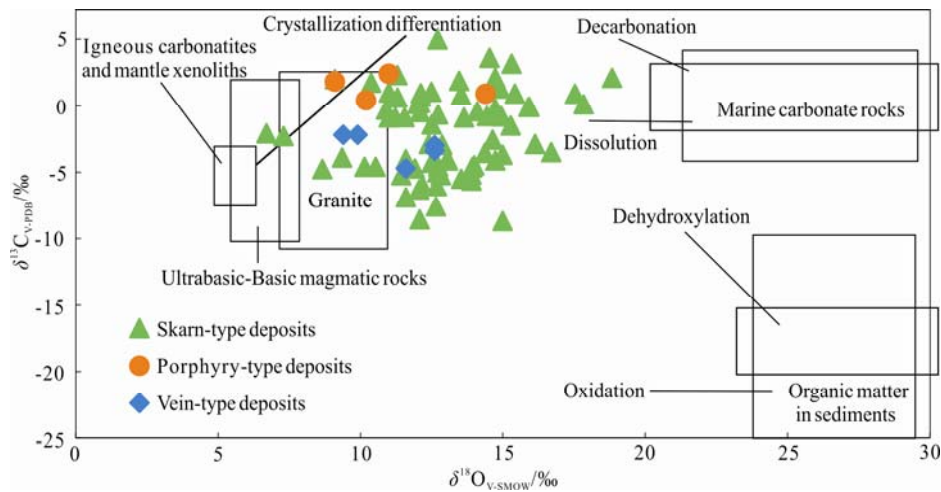


Fig. 13. $\delta^{18}\text{O}$ (‰) vs. $\delta^{13}\text{C}$ (‰) diagrams for the ore minerals from the major deposits in the Tongling ore district. Data sources: the carbon and oxygen isotope compositions of vein-type deposits are represented by the Yaojialing (Liu Shaofeng, 2012) and Baocun deposits (Pan Zhijun, 1992). Porphyry-type ores are from the deeper Hucunna (this paper). Skarn-type ores are cited from Dongguashan (Liu Yuqing and Liu Zhaolian, 1991; Huang Shunsheng et al., 2003; Xu Zhaowen et al., 2007; Lu Sanming, 2007); Shizishan (Xiao Xinjian et al., 2002; Gu Lianxing and Chen Peirong, 2002); Chaoshan (Tian Shihong et al., 2004; Gao Geng et al., 2006; Wang Jianzhong et al., 2008); Tongguashan (Liu Yuqing and Liu Zhaolian, 1991; Tian Shihong et al., 2005); Xinqiao (Liu Yuqing and Liu Zhaolian, 1991).

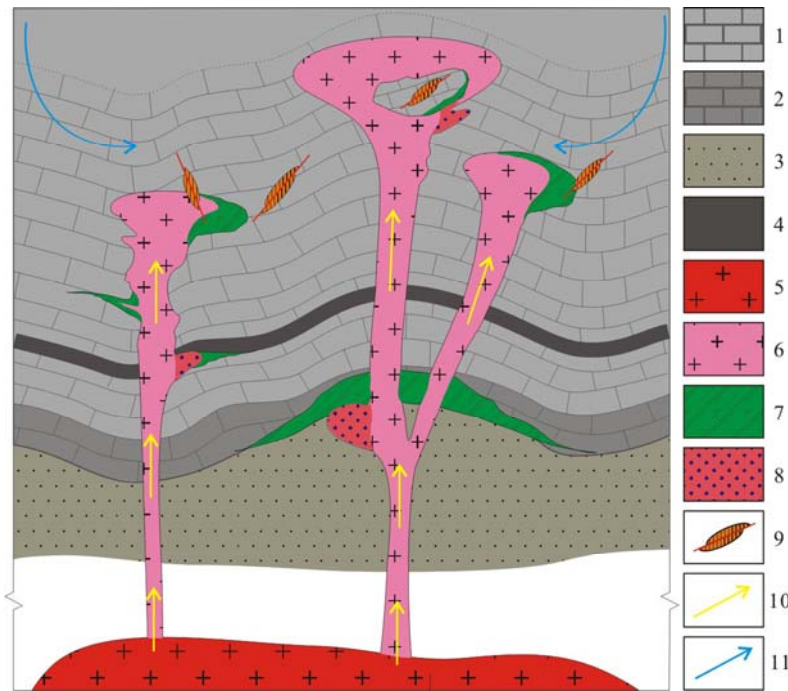


Fig. 14. Metallogenic model of polymetallic copper-gold deposits in the Tongling ore district
1, Permian-Triassic carbonate rocks; 2, Carboniferous carbonate rocks; 3, Silurian-Devonian sandstones, siltstones; 4, sillalites; 5, deep-set magma chamber; 6, intermediate-acid intrusions; 7, skarn-type deposits; 8, porphyry-type deposits; 9, vein-type deposits; 10, magmatic water; 11, meteoric water.

relationship between these orebodies and Yanshanian magmatism. This relationship led Chang Yinbo and Liu Xuegui (1983) to suggest that the Dongguashan deposit represents a stratabound skarn-type deposit. Mao Jingwen et al. (2009) considered that the laminated structure of the Dongguashan ores was caused by the alteration of magnesian skarns, a model that is consistent with the presence of serpentinized olivine in this area. Then Xu Xiaochun et al. (2010) used the Ohmoto model (Ohmoto

and Rye, 1979) to determine the source of sulfur in the upper Dongguashan deposit, indicating that the sulfur of these stratiform orebodies should be derived from Yanshanian magma. Huang Shunsheng et al. (2003) also suggested that the Cu isotopic composition of the mineralization within the stratiform orebodies of the Dongguashan deposit was indicative of derivation from a magmatic source. Combining these with the similar isotopic geochemical compositions of the different types

of deposits in the Tongling district suggests that all of them were generated by a unified magmatic–hydrothermal system.

The Tongling ore district is one of the largest polymetallic copper–gold ore districts within the MLYB and hosts numerous well-known skarn deposits (Tang Yongcheng et al., 1998; Pan and Dong, 1999; Huang Chongke et al., 2001; Zhang et al., 2017). Recent research has indicated that this district also contains porphyry- and vein-type deposits as well as systems that contain two or three of these different types of deposit. All of these deposits are associated with Yanshanian magmatism and hydrothermal activity. Here, we propose a model for the generation of these porphyry–skarn–vein-type deposits as a result of the formation of a unified magmatic–hydrothermal system. This model provides a theoretical basis to guide further exploration for deep-seated porphyry Cu–(Mo, Au) and shallow vein Au, Ag, and Pb–Zn deposits in the Tongling ore district as well as insights for future research into the metallogenesis of this and adjacent districts.

5 Conclusions

(1) The Tongling ore district is important in the MLYB for its numerous polymetallic copper–gold deposits, and is well-known in the world for its typical skarn-type deposits. The geological characteristics of the deposits discovered recently in this ore district indicate that it also contains a lot of porphyry- and vein-type deposits as well as deposits that have characteristics that appear to be combinations of these types. All these types of deposits are closely linked in terms of spatial distribution and the zoning of ore-forming elements.

(2) The polymetallic copper–gold deposits in the Tongling ore district are clearly spatially and temporally related to Yanshanian pyroxene diorite, quartz diorite, and granodiorite intrusions. Geochemical characteristics of fluid inclusions and stable isotopes indicate that the ore-forming fluids, metals and associated elements of these deposits in the ore district were generally derived from the intermediate–acid granitic magma, with comparatively minor contributions from the surrounding sedimentary rock.

(3) The porphyry-, skarn-, and vein-type deposits in the Tongling ore district appear to have formed from a unified magmatic–hydrothermal system. This study presents a new genetic model for these porphyry–skarn–vein deposits. It also provides a basis for further research on and exploration for deep-seated porphyry-type Cu–(Mo, Au) deposits and the associated shallow vein Au, Ag, and Pb–Zn deposits in this district that builds on the intensive research and exploration undertaken on the skarn-type deposits within the Tongling ore district.

Acknowledgements

This study was funded by the National Natural Science Foundation of China (NSFC) (grant numbers 41472066, 40972063 and 41672038), the Program of the Deep Exploration in China (SinoProb-03-05), the National Key

R&S Program of China (2016 YFC0600209) and the Land and Resources Science and Technology Foundation of Anhui Province (2016-K-03 and No. 2014-K-03).

Manuscript received Mar. 10, 2018

accepted Oct. 12, 2018

associate EIC MAO Jingwen

edited by FEI Hongcai

References

- Cao, Y., Du, Y.S., Pang, Z.S., Du, Y.L., Kou, S.L., Chen, L.J., Gao, F.P., and Zhou, G.B., 2015. Geologic, Fluid Inclusion and Stable Isotope Constraints on Mechanisms of Ore Deposition at the Datuanshan Copper Deposit, Middle-Lower Yangtze Valley, Eastern China. *Acta Geologica Sinica* (English Edition), 89(3): 746–765.
- Cao, Y., Zheng, Z. J., Du, Y.L., Cao, F.P., Qin, X.L., Yang, H.M., Lu, Y.H., and Du, Y.S., 2017. Ore geology and fluid inclusions of the Hucunnan deposit, Tongling, Eastern China: Implications for the separation of copper and molybdenum in skarn deposits. *Ore Geology Reviews*, 81: 925–939.
- Chang Yinbo and Liu Xuegui, 1983. On strata-bound skarn deposits. *Mineral Deposits*, 2(2): 11–20 (in Chinese with English abstract).
- Chang Yinbo, Liu Xiangpei and Wu Yanchang, 1991. *The Copper–Iron Belt of the Lower and Middle Reaches of the Changjiang River*. Beijing: Geological Publishing House, 379 (in Chinese).
- Chu Guozheng and Li Dongxu, 1992. Bedding slipping structures control on the “Multistorey” ore deposits, in the Shizishan orefield of Anhui. *Geoscience*, 6(4): 504–512.
- Chu Guozheng, 2003. *The metallogenic system and its implications for deposit exploration in the Cu and Au ore field of Shizishan, Tongling*. Beijing: China University of Geosciences (Ph. D thesis): 1–149.
- Deng Jinfu, Dai Shengqian, Zhao Hailing and Du Jianguo, 2002. Recognition of magmatic–fluid–metallogenic systems and subsystems in Tongling Cu–Au (Ag) ore-forming area. *Mineral Deposits*, 21(4): 317–322 (in Chinese with English abstract).
- Deng, J., Wang, Q.F., Xiao, C., Yang, L., Liu, H., Gong, Q., and Zhang, J., 2011. Tectonic–magmatic–metallogenic system, Tongling ore cluster region, Anhui Province, China. *International Geology Review*, 53(5–6): 449–476.
- Du Jingguo, Du Yangsong, Chen Linjie and Pang Zhenshan, 2016. Magmatic processes in Jiaochong gold deposit, Tongling, China: Evidence from dioritic porphyrite. *Earth Science Frontiers*, 23(3): 221–229 (in Chinese with English abstract).
- Du, Y.L., Deng, J., Cao, Y., and Li, D.D., 2015. Petrology and geochemistry of Silurian–Triassic sedimentary rocks in the Tongling region of Eastern China: their roles in the genesis of large stratabound skarn ore deposits. *Ore Geology Reviews*, 67: 255–263.
- Duan, L.A., Gu, H.L., Yang, X.Y., 2017. Geological and geochemical constraints on the newly discovered Yangchongli gold deposit in Tongling region, Lower Yangtze Metallogenic Belt. *Acta Geologica Sinica* (English Edition), 91(6): 2078–2108.
- Duan, L.A., Yang, X.Y., Deng, J.H., Wang, F.Y., and Lee, I.S., 2018. Mineralization, geochemistry and zircon U–Pb ages of the Paodaoling porphyry gold deposit in the Guichi region, Lower Yangtze Metallogenic Belt, Eastern China. *Acta Geologica Sinica* (English Edition), 92(2): 706–732.
- Edwards, R.P., and Atkinson, K., 1986. *Ore deposit geology and its influence on mineral exploration*. London: Chapman and Hall, 466.
- Fan Ziliang, Xu Xiaochun, Chen Linjie, He Jun and Xie Qiaolin, 2016. The geological features and metallogenic setting of the porphyry copper–molybdenum–gold deposits in Tongling ore district, Anhui Province. *Acta Petrologica Sinica*, 32(2): 351–368 (in Chinese with English abstract).
- Gu Lianxing and Xu Keqin, 1986. On the carboniferous

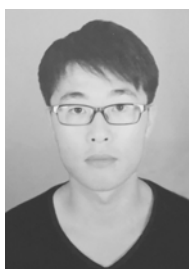
- submarine massive sulphide deposits in the lower reaches of the Changjiang (Yangzi) River. *Acta Geologica Sinica*, (2): 176–189 (in Chinese with English abstract).
- Gu Lianxing and Chen Peirong, 2002. Comparative research on ore-forming fluids for the main types of hydrothermal copper-gold deposits in the Middle and Lower Reaches the Yangtze River. *Journal of Nanjing University (Natural Sciences)*, 38 (3): 392–407 (in Chinese with English abstract).
- Gu, L.X., Zaw, K., Hu, W.X., Zhang, K.J., Ni, P., He, J.X., Xu, Y.T., Lu, J.J., and Lin, C.M., 2007. Distinctive features of Late Palaeozoic massive sulphide deposits in South China. *Ore Geology Reviews*, 31(1–4): 107–138.
- Guo Weiming, 2010. *Superimposed Mineralization of the Dongguashan Deposit at the Tongling, Anhui Province, and Geochemistry and Mineralogy of Associated Intrusions*. Nanjing: Nanjing University (Ph. D thesis): 1–100.
- Guo Weiming, Lu Jianjun, Jiang Shaoyong, Zhang Rongqing and Qi Liang, 2011. Re-Os isotope dating of pyrite from the footwall mineralization zone of the Xinqiao deposit, Tongling, Anhui Province: Geochronological evidence for submarine exhalative sedimentation. *Chinese Science Bulletin*, 56: 3860–3865 (in Chinese).
- Guo Wenkui, 1957. On the genesis of the Tongguanshan copper deposit. *Acta Geologica Sinica*, 37(3): 317–332 (in Chinese with English abstract).
- Guo Zongshan, 1957. Some skarn copper deposits in Lower Yangtze River valley. *Acta Geologica Sinica*, 37(1): 1–10 (in Chinese with English abstract).
- Hou Zengqian, Yang Zhusheng, Tian Lvqing, Zeng Pusheng, Xie Yuqing, Meng Yifeng, Hong Tianshi, Xu Wenyi, Li Hongyang and Jiang Zhangping, 2011. The large-scale Dongguashan deposit, Shizishan district in east China: Carboniferous sedex-type massive sulfides overprinted by late Jurassic skarn Cu mineralization. *Acta Geologica Sinica*, 85(5): 659–686 (in Chinese with English abstract).
- Hu Huan, Wang Rucheng, Lu Jianjun and Liu Guanghua, 2001. Mineral association, chemical composition and genetic significance of skarn gold deposits in the Shizishan orefield, Tongling Area, Anhui Province. *Mineral Deposits*, 20(1): 86–98 (in Chinese with English abstract).
- Huang Bin, 1991. Pb isotopic studies of the massive sulphur-iron-gold deposits in the Tongling district, Anhui Province. *Acta Geologica Sinica*, 4: 347–359 (in Chinese with English abstract).
- Huang Chongke, Bai Ye, Zhu Yusheng, Wang Huizhang and Shang Xiuzhi, 2001. Copper deposit of China. Beijing: Geology Publishing House, 371 (in Chinese).
- Huang Shunsheng, Xu Zhaowen and Ni Pei, 2003. Inclusion geochemistry of Dongguashan hydrothermal superimposition copper deposit in the Tongling area, Anhui. *Contributions of Geology and Mineral Resources Research*, 18(1): 34–38 (in Chinese with English abstract).
- Ishihara, S., 1981. The granitoid series and mineralization. *Economic Geology*, 75th Anniversary Volume: 458–484.
- Jiang Qisheng, Han Changsheng and Huang Jianman, 2005. Geological features of the copper-lead-zinc deposit in yaojialing and its genetic discussion. *Geology of Anhui*, 15(4): 265–269 (in Chinese with English abstract).
- Jiang Qisheng, Zhao Zihong and Huang Jianman, 2008. Discovery of the Yaojialing copper-lead-zinc deposit in Nanlin, Anhui, and its significance. *Geology in China*, 35(2): 314–321 (in Chinese with English abstract).
- Li Jinwen, 2004. *Ore-controlling structure of orefield and ore-forming chemical kinetics of mineral assemblage area in Tongling*. Beijing: Chinese Academy of Geological Sciences (Ph. D thesis): 1–142.
- Li Wenda, 1989. On the Yangtze type copper ore deposits and their origin. *Bulletin of the Nanjing Institute Geology and Mineral Resources, Chinese Academy Geological Sciences*, 10 (2): 1–14 (in Chinese with English abstract).
- Li Wenda, Mao Jianren, Zhu Yunhe and Xie Huaguang, 1998. *Mesozoic igneous rocks and ore deposits in southeast China*. Beijing: Seismological Publishing House, 159 (in Chinese).
- Liu Guangxian, Yuan Feng, Deng Yufeng, Sun Weian, Yang Di and Li Xiansuo, 2017. Geochronology, geochemistry and geological characteristics of the diorite from Hehuashan zinc-lead deposit, Tongling, Anhui Province. *Acta Petrologica Sinica*, 33 (11): 3581–3598 (in Chinese with English abstract).
- Liu Shaofeng, 2012. *The metallogenic research of Yaojialing Zn-Au polymetallic deposit in Tongling, Anhui Province*. Beijing: China University of Geosciences (Ph. D thesis): 1–139.
- Liu Wencan and Li Dongxu, 1993. The deformation characteristics of folding structures and their interfering depths in the Tongling area of Anhui. *Geology of Anhui*, 3: 1–9 (in Chinese with English abstract).
- Liu Wencan, Li Dongcu and Gao Dezhen, 1996. Analysis of the time sequence of compounding structural deformation systems and the resulting effects in Tongling area. *Journal of Geomechanics*, 2(1): 42–48 (in Chinese with English abstract).
- Liu Xiaoming, 2016. Geological features and mineralization law of the hehuashan Pb-Zn-Ag polymetallic ore deposit in Tongling County, Anhui Province. *Geology of Anhui*, 26: 189–193 (in Chinese with English abstract).
- Liu Yuqing and Liu Zholian, 1991. Isotope geochemistry and genesis of the stratiform copper (iron-sulfur) deposits in Tongling area, Anhui Province. *Bulletin of Institute Mineral Research, Chinese Academy of Geological Sciences* 1, 47–114 (in Chinese with English abstract).
- Liu Yuqing, Liu Zholian and Yang Chengxing, 1984. Stable isotope studies of the Dongguashan copper deposit in Tongling Prefecture, Anhui Province. *Bulletin of the Institute of Mineral Deposits, Chinese Academy of Geological Sciences* 1, 70–101 (in Chinese with English abstract).
- Liu Zhongfa, Shao Yongjun, Zhou Xin, Zhang Yu and Zhou Guibin, 2014. Hydrogen, oxygen, sulfur and lead isotope composition tracing for the ore-forming material source of Dongguashan copper (gold) deposit in Tongling, Anhui Province. *Acta Petrologica Sinica*, 30 (1): 199–208 (in Chinese with English abstract).
- Lou Jinwei, 2012. *Intermediate-Acid Intrusive Rocks of Tongling Ore District and Copper-Polymetallic Deposits of Shizishan Ore-Field, Anhui Province*. Hefei: Hefei University of Technology (Ph. D thesis): 1–223.
- Lu Jianjun, Guo Weimin, Chen Weifeng, Jiang Shaoyong, Li Juan, Yan Xiaorong and Xu Zhaowen, 2008. A metallogenic model for the Dongguashan Cu-Au deposit of Tongling, Anhui Province. *Acta Petrologica Sinica*, 24(8): 1857–1864 (in Chinese with English abstract).
- Lu Sanming, 2007. *The magmatism and fluid mineralization in Shizishan copper-gold district in Tongling, Anhui Province*. Hefei: Hefei University of Technology (Ph. D thesis): 1–132.
- Ma Xingyuan and He Guoqi, 1989. Precambrian crustal evolution of eastern Asia. *Journal of Southeast Asian Earth Sciences*, 3(1–4): 9–15 (in Chinese with English abstract).
- Mao Jingwen, Holly Stein, Du Andao, Zhou Taofa, Mei Yanxiong, Li Yongfeng, Zang Wenshuan and Li Jingwen, 2004. Molybdenite Re-Os precise dating for molybdenite from Cu-Au-Mo deposits in the Middle-Lower Reaches of Yangtze River belt and its implications for mineralization. *Acta Geologica Sinica*, 78(1): 121–131 (in Chinese with English abstract).
- Mao Jingwen, Shao Yongjun, Xie Guiqing, Zhang Jiandong and Chen Yuchuan, 2009. Mineral deposit model for porphyry-skarn polymetallic copper deposits in Tongling ore dense district of Middle-Lower Yangtze Valley metallogenic belt. *Mineral Deposits*, 28(2): 109–119 (in Chinese with English abstract).
- Mao, J.W., Wang Y.T., Lehmann, B., Yu, J.J., Du, A.D., Mei, Y.X., Li, Y.F., Zang, W.S., Stein, H.J., and Zhou, T.F., 2006. Molybdenite Re-Os and albite $^{40}\text{Ar}/^{39}\text{Ar}$ dating of Cu-Au-Mo and magnetite porphyry systems in the Yangtze River valley and metallogenic implications. *Ore Geology Reviews*, 29(3): 307–324.
- Mao, J.W., Xie, G.Q., Duan, C., Franco, P., Dazio, I., and Chen, Y.C., 2011. A tectono-genetic model for porphyry-skarn-stratabound Cu-Au-Fe and magnetite-apatite deposit along the Middle-Lower Yangtze River Valley, Eastern China. *Ore Geology Reviews*, 43: 294–314.
- Mcculloch M.T., and Chappell B.W., 1982. Nd isotopic

- characteristics of S- and I-type granites. *Earth & Planetary Science Letters*, 58(1): 51–64.
- Meng Xianming, 1963. *Classification of mineral deposits and exploration strategy*. In: *Classification and Genesis of Mineral Deposits*. Beijing: Science Press, 72 (in Chinese).
- Meng Yifeng, Yang Zhusen, Zeng Pusheng, Xu Wenyi and Wang Xunwei, 2004. Tentative temporal constraints of ore-forming fluid systems in Tongling metallogenic province. *Mineral Deposits*, 23(3): 271–280 (in Chinese with English abstract).
- Ohmoto, H., and Rye, R.O., 1979. Isotopes of sulfur and carbon. *Geochemistry of Hydrothermal Ore Deposit*: 509–567.
- Pan, Y.M., and Dong, P., 1999. The Lower Changjiang (Yangzi/Yangtze River) metallogenic belt, east central China: intrusion - and wall rock-hosted Cu–Fe–Au, Mo, Zn, Pb, Ag deposits. *Ore Geology Reviews*, 15(4): 177–242.
- Pan Zhijun, 1992. *The geological features of Longhushan gold deposit, Tongling, Anhui Province*. Beijing: Chinese University of Geosciences (M.S. thesis).
- Qu Hongying, Pei Rongfu, Wang Haolin, Li Jinwen, Wang Yonglei and Mei Yanxiong, 2011. Mantle-derived ore-forming fluids of the Fenghuangshan Cu deposit, evidences from microthermometric and isotopic studies. *Geological Review*, 57(1): 50–62 (in Chinese with English abstract).
- Qu, H.Y., Pei, R.F., Fei, H.C., Li, J.W., Wang, Y.L., Wang, H.L., and Yao, L., 2012. Geology, geochemistry, and geochronology of the Fenghuangshan skarn-type copper deposit in the Tongling ore cluster, Anhui Province, east China. *Acta Geologica Sinica* (English Edition), 86(3): 700–718.
- Que Chaoyang, Wu Ganguo, Zhang Da, Zhang Zhihui, Di Yongjun, Fang Hongwei and Yuan Qin, 2013. LA-ICP-MS zircon U–Pb dating of dioritic porphyrite in Jiaochong Au–S deposit, Tongling area, and its geological significance. *Mineral Deposits*, 32(6): 1221–1235 (in Chinese with English abstract).
- Ren Yunsheng, Liu Liandeng and Wan Xiangzong, 2006. Geological characteristics and genesis of the Baocun gold deposit in Tongling Area, Anhui Province. *Acta Geoscientia Sinica*, 27 (6): 583–589 (in Chinese with English abstract).
- Shao Yongjun, Peng Shenglin, Lai Jianqing, Liu Liangming, Zhang Yizhou and Zhang Jiandong, 2007. Identification of two types of mineralized intrusion in the Fenghuangshan copper deposit and analysis of their genesis. *Acta Petrologica Sinica*, 23(10): 2471–2482.
- Tang Yongcheng, Wu Yanchang, Chu Guozheng, Xing Fengming, Wang Yongmin, Cao Fengyang and Chang Yinuo, 1998. *Geology of copper-gold polymetallic deposits in the along-Changjiang area of Anhui Province*, Beijing: Geological Publishing House, 351 (in Chinese).
- Taylor B.E., 1986. Magmatic volatiles; isotopic variation of C, H, and S. *Mineralogical Society of America*, 16(1): 185–225.
- Taylor, H.P., and Forester, R.W., 1979. An Oxygen and Hydrogen Isotope Study of the Skaergaard Intrusion and its Country Rocks: a Description of a 55 M.Y. Old Fossil Hydrothermal System. *Journal of Petrology*, 20: 287–296.
- Tian Shihong, Ding Tiping, Hou Zengqian, Yang Zhusen, Xie Yuling, Wang Yanbin and Wang Xuncheng, 2005. REE and stable isotope geochemistry of the Xiaotongguanshan copper deposit, Tongling, Anhui. *Geology in China*, 32(4): 604–613 (in Chinese with English abstract).
- Tian Shihong, Ding Tiping, Yang Zhusen, Meng Yifeng, Zeng Pusheng, Wang Yanbin, Wang Xuncheng and Jiang Zhangping, 2004. REE and stable isotope geochemical characteristics of Chaoshan gold deposit in Tongling, Anhui Province. *Mineral Deposits*, 23(3): 365–374 (in Chinese with English abstract).
- Wang Hongzhen and Mo Xuanxue, 1995. An outline of the tectonic evolution of China. *Episodes*, 18: 6–16 (in Chinese with English abstract).
- Wang J. Z., Li J.W., Zhao X.F., Ma C.Q., Qu W.J., and Du A.D., 2008. Re–Os Dating of Pyrrhotite from the Chaoshan Gold Skarn, Eastern Yangtze Craton, Eastern China. *International Geology Review*, 50(4): 392–406.
- Wang Jianzhong, Li Jianwei, Zhao Xinfu, Qian Zhuangzhi and Ma Changqian, 2008. Genesis of the Chaoshan gold deposit and its host intrusion, Tongling area: constraints from $^{40}\text{Ar}/^{39}\text{Ar}$ ages and elemental and Sr–Nd–O–C–S isotope geochemistry. *Acta Petrologica Sinica*, 24 (8): 1875–1888 (in Chinese with English abstract).
- Wang Shiwei, 2015. *Porphyry deposits and associated magmatic activity in the Anhui segment of the Middle-Lower Yangtze River Valley metallogenic belt*. Hefei: Hefei University of Technology (Ph. D thesis): 1–251.
- Wang Shiwei, Zhou Taofa, Yuan Feng, Fan Yu, Cao Xiaosheng and Wang Biao, 2012. Re–Os and $^{40}\text{Ar}/^{39}\text{Ar}$ dating of the Shujiadian copper deposit in Tongling, China: Implications for regional metallogenesis. *Acta Petrologica Sinica*, 28: 3170–3180 (in Chinese with English abstract).
- Wang Yangyang, Xiao YiLin and Yang Xiaoyong, 2015. Re–Os isotope systematics and fluid inclusions of Xinqiao deposit in Tongling, the Middle-Lower Yangtze River Metallogenic Belt. *Acta Petrologica Sinica*, 31: 1031–1039 (in Chinese with English abstract).
- Wang, Q.F., Deng, J., Huang, D.H., Xiao, C.H., Yang, L.Q., and Wang, Y.R., 2010. Deformation model for the Tongling ore cluster region, east-central China. *International Geology Review*, 53(5–6): 562–579.
- Wang, Q.F., Deng, J., Huang, D.H., Xiao, C.H., Yang, L.Q., and Wang, Y.R., 2011. Deformation model for the Tongling ore cluster region, east-central China. *International Geology Review*, 53: 562–579.
- Wang, S.W., Zhou, T., Yuan, F., Fan, Y., White, N.C., and Lin, F., 2014. Geological and geochemical studies of the Shujiadian porphyry Cu deposit, Anhui Province, Eastern China: Implications for ore genesis. *Journal of Asian Earth Sciences*, 103: 252–275.
- Wang, S.W., Zhou, T.F., Yuan, F., Fan, Y., Zhang, L.J., and Song, G.X., 2015. Petrogenesis of Dongguashan skarn-porphyry Cu–Au deposit related intrusion in the Tongling district, eastern China: Geochronological, mineralogical, geochemical and Hf isotopic evidence. *Ore Geology Reviews*, 64: 53–70.
- Wen Chunhua, Xu Wenyi, Zhong Hong, Lv Qingtian, Yang Zhusen, Tian Shihong and Liu Yingchao, 2011. Geological characteristics and fluid inclusion studies of shallow mineralization in Yaojialing Zn–Au–polymetallic deposit, Anhui Province. *Mineral Deposits*, 30(3): 533–546 (in Chinese with English abstract).
- Wu Cailai, Dong Shuwen and Guo Xiangyan, 2013. *Intermediate-Acid Intrusive Rocks from Tongling, China*, Beijing: Geological Publishing House, 220 (in Chinese).
- Wu Cailai, Dong Shuwen, Guo Heping, Guo Xiangyan, Gao Qianming, Liu Lianggen, Chen Qilong, Lei Min, Wooden, J.L., Mazadab, F.K., and Mattinson, C., 2008. Zircon SHRIMP U–Pb dating of intermediate-acid intrusive rocks from Shizishan, Tongling and the deep processes of magmatism. *Acta Petrologica Sinica*, 24(8): 1801–1812 (in Chinese with English abstract).
- Wu Cailai, Gao Qianming, Guo Heping, Guo Xiangyan, Liu Liaogen, Hao Yuanhong, Lei Min, Qin Haipeng and Chen Qilong, 2010. Zircon SHRIMP dating of intrusive rocks from the Tongguashan ore-field in Tongling, Anhui, China. *Acta Geologica Sinica*, 84(12): 1746–1758 (in Chinese with English abstract).
- Wu Ganguo, Zhang Da and Zang Wenshan, 2003. Study of tectonic layering motion and layering mineralization in the Tongling metallogenic cluster. *Sciences in China, Series D*, 33 (4): 300–308 (in Chinese).
- Wu Yanchang and Chang Yinuo, 1998. On the magmatic skarn. *Earth Science Frontiers*, 5(4): 291–301 (in Chinese with English abstract).
- Wu Yanchang, 1992. On magmatic skarn—a new type of skarn. *Geology of Anhui*, 2(1): 12–26 (in Chinese with English abstract).
- Wu Yanchang, Shao Guiqing and Wu Lian, 1996. Magmatic skarn and its ore deposits. *Geology of Anhui*, 6(2): 30–39 (in Chinese with English abstract).
- Xiao Xinjian, Gu Lianxing and Ni Pei, 2002. Multi-episode fluid boiling in the Shizishan copper-gold deposit at Tongling, Anhui Province: Its bearing on ore-forming. *Science in China (Series D)*, 45 (1): 34–44 (in Chinese).
- Xie Guiqing, Zhu Qiao, Yao Lei, Wang Jian and Li Wei, 2013.

- Discussion on regional metal mineral deposit model of Late Mesozoic Cu-Fe-Au polymetallic deposits in the southeast Hubei Province. *Bulletin of Mineralogy, Petrology and Geochemistry*, 32 (4): 418–426 (in Chinese with English abstract).
- Xie Jiancheng, 2008. *The diagenesis and metallogenesis research of Mesozoic magmatic rocks in Tongling region, Anhui Province*. Hefei: University of Science and Technology of China (Ph. D thesis): 213.
- Xie Zhi, Sun Weidong, Chai Zhifang, Chen Jiangfeng, Du Andao, Li Chunsheng and Mao Xueying, 2002. Comparison of Os-Os and Re-Os dating results of molybdenites. *Nuclear Techniques*, 25(12): 1013–1018 (in Chinese with English abstract).
- Xie, J.C., Yang, X.Y., Sun, W.D., Du, J.G., Xu, W., Wu, L.B., Wang, K.Y., and Du, X.W., 2009. Geochronological and geochemical constraints on formation of the Tongling metal deposits, middle Yangtze metallogenic belt, east-central China. *International Geology Review*, 51(5): 388–421.
- Xing Fengming and Xu Xiang, 1996. High-potassium calc-alkaline intrusive rocks in Tongling area, Anhui Province. *Acta Geologica Sinica*, 25(1): 29–38 (in Chinese with English abstract).
- Xing Fengming, Zhao Bin, Xu Xiang, Zhu Chengming, Zhao Jinsong and Cai Enzhao, 1997. Experimental study on the genesis of intrusive rocks in the Tongling area, Anhui. *Regional Geology in China*, 16: 267–274 (in Chinese with English abstract).
- Xu Keqin and Zhu Jinchu, 1978. The Origin of the sedimentary (or Volcano sedimentary) iron copper deposits in some fault depression belts in Southeast China. *Fujian Geology*, 4: 1–68 (in Chinese).
- Xu Xiaochun, Bai Ruyu, Xie Qiaoqin, Lou Jinwei, Zhang Zhanzhan, Liu Qineng and Chen Liwei, 2012. Re-understanding of the geological and geochemical characteristics of the Mesozoic intrusive rocks from Tongling area of Anhui Province, and discussions on their genesis. *Acta Petrologica Sinica*, 28(10): 3139–3169 (in Chinese with English abstract).
- Xu Xiaochun, Fan Ziliang, He Jun, Liu Xue, Liu Xiaoyan, Xie Qiaoqin, Lu Sanming and Lou Jinwei, 2014. Metallogenic model for the copper-gold polymetallic deposits in Shizishan ore field, Tongling, Anhui Province. *Acta Petrologica Sinica*, 30(4): 1054–1074 (in Chinese with English abstract).
- Xu Xiaochun, Fan Ziliang, Wang Meng, Fu Zhongyang, He Jun and Xie, Qiaoqing, 2018a. Two types of zircons from the Jiaochong pyroxene diorite pluton in the Tongling area of Anhui Province and their geological significance. *Acta Geologica Sinica*, 92 (1): 28–40 (in Chinese with English abstract).
- Xu Xiaochun, Lou Jinwei, Liang Jianfeng, Xiao Qiuxiang, Zhang Zanzan, Liu Qineng and Wang Ping, 2011. Latest progress in ore deposit exploration and geological research in the Tongling ore concentration area, Anhui. *Geology of Anhui*, 21(2): 119–130 (in Chinese with English abstract).
- Xu Xiaochun, Lu Sanming, Xie Qiaoqin, Bai Lin and Chu Guozheng, 2008. SHRIMP zircon U-Pb dating for the magmatic rocks in Shizishan ore-field of Tongling, Anhui Province, and its geological implications. *Acta Geologica Sinica*, 82(4): 500–509 (in Chinese with English abstract).
- Xu Xiaochun, Yin Tao, Lou Jinwei, Lu Sanming, Xie Qiaoqin and Chu Pingli, 2010. Origin of Dongguashan stratabound Cu-Au Skarn deposit in Tongling: restraints of sulfur isotope. *Acta Petrologica Sinica*, 26(9): 2739–2750 (in Chinese with English abstract).
- Xu Xiaochun, Zuo Xu, He Jun and Fu Zhongyang, 2018b. Geological and geochemical characteristics of the intrusive rocks of early and late stages during Late Mesozoic in Tongling district, Anhui Province. *Geological Journal of China Universities*, 24 (3): 325–339 (in Chinese with English abstract).
- Xu Zhaowen, Huang Shensheng, Ni Pei, Lu Xiancai and Lu Jianjun, 2005. Characteristics and evolution of ore fluids in Dongguashan copper deposit, Anhui Province, China. *Geological Review*, 51(1): 36–41 (in Chinese with English abstract).
- Xu Zhaowen, Lu Xiancai, Gao Geng, Fang Changquan, Wang Yunjian, Yang Xiaonan, Jiang Shaoyong and Chen Bangguo, 2007. Isotope geochemistry and mineralization in the dongguashan diplogenetic stratified copper deposit, Tongling area. *Geological Review*, 53(1): 44–51 (in Chinese with English abstract).
- Xu, G., and Zhou, J., 2001. The Xinqiao Cu–Au–S deposit in the Tongling mineral district, China: synorogenic remobilization of a stratiform sulfide deposit. *Ore Geology Reviews*, 18 (1): 77–94.
- Xu, X.C., Zhang, Z.Z., Liu, Q.N., Lou, J.W., Xie, Q.Q., Chu, P.L., and Frost, R.L., 2011. Thermodynamic study of the association and separation of copper and gold in the Shizishan ore field, Tongling, Anhui Province, China. *Ore Geology Reviews*, 43(1): 347–358.
- Yang Gang, Chen Jiaofeng, Du Andao, Qu Wenjun and Yu Gang, 2004. Re-Os dating of Mo-bearing black shale of the Laoyaling deposit, Tongling, Anhui Province, China. *Chinese Science Bulletin*, 49(12): 1205–1208 (in Chinese with English abstract).
- Yang H.M., Du Y.S., Lu Y.H., Chen L.J., Zheng Z.J., and Zhang Y., 2016. U–Pb and Re–Os Geochronology of the Hucunnan Copper–Molybdenum Deposit in Anhui Province, Southeast China, and its Geological Implications. *Resource Geology*, 66 (3): 303–312.
- Yang Heming, 2016. *Characteristics and Genesis of the Hucunnan Polygenetic Compound Cu-Mo Deposit, Tongling, Anhui Province*. Beijing: China University of Geosciences (Ph. D thesis): 1–91.
- Yang Qiurong, Wang Jinfang, Feng Jingzhi, Hou Zengqian, Yang Zhusen, Meng Yifeng, Wang Songying and Chen Wentao, 2010. Geological and geochemical characteristics of the Tianmashan Au-S deposit in Tongling, Anhui Province. *Acta Geoscientica Sinica*, 31(2): 203–208 (in Chinese with English abstract).
- Yang Zhusen, Hou Zengqian, Meng Yifeng, Zeng Pusheng, Li Hongyang, Xu Wenyi, Tian Shihong, Wang Xuncheng, Yao Xiaode and Jiang Zhangping, 2004. Spatial-temporal structure of Hercynian exhalative-sedimentary fluid system in Tongling ore concentration area, Anhui Province. *Mineral Deposits*, 23 (3): 281–297 (in Chinese with English abstract).
- Yin Yanduan, Hong Tianqiu, Jia Zhihai, Zhao Huan, Li Chao, Luo Lei and Huang Jianman, 2016. The Re-Os age of molybdenite and ore-forming material source from the Yaojialing Zn-Au polymetallic deposit, Tongling. *Geological Review*, 62(1): 248–255 (in Chinese with English abstract).
- Yuan Feng, Song Yulong, Wang Shiwei, Zhou Taofa and Sun Weian, 2014. Characteristics of porphyry mineralization in the depth of Dongguashan deposit and its relationship with skarn-type mineralization. *Chinese Journal of Geology*, 49(2): 588–607 (in Chinese with English abstract).
- Yue Zilong, 2015. *Characteristics and genesis of the Guihuachong copper deposit in Anhui Province*. Beijing: China University of Geosciences (Ph D thesis): 1–112.
- Zang Wenshan, Wu Ganguo, Zhang Da, Zhang Xiangxin, Li Jinwen, Liu Aihua and Zhang Zhongyi, 2007. A preliminary discussion on genesis of Xinqiao S-Fe orefield. *Mineral Deposits*, 26: 464–474 (in Chinese with English abstract).
- Zeng Pusheng, Pei Rongfu, Hou Zengqian, Meng Yifeng, Yang Zhusen, Tian Shihong, Xu Wenyi and Wang Xuncheng, 2005. The Dongguashan Deposit in the Tongling Mineralization Cluster Area, Anhui: A Large-sized Superimposition-type Copper Deposit. *Acta Geologica Sinica*, 79(1) 106–113 (in Chinese with English abstract).
- Zeng Pusheng, Yang Zhusen, Meng Yifeng, Pei Rongfu, Wang Yanbin, Wang Xuncheng, Xu Wenyi, Tian Shihong and Yao Xiaode, 2004. Temporal-spatial Configuration and Mineralization of Yanshanian Magmatic Fluid Systems in Tongling Ore Concentration Area, Anhui Province. *Mineral Deposits*, 23(3): 298–309 (in Chinese with English abstract).
- Zhai Yusheng, Yao Shuzhen and Lin Xinduo 1992. *Metallogenic Regularity of Fe-Cu (-Au) in the Middle-Lower Reaches of the Yangtze-River Area*, Beijing: Geological Publishing House, 235 (in Chinese).

- Zhan Changfan, 2013. *Studies on the geology and ore-forming fluids of the Yaojialing Cu-polymetallic deposit in Anhui Province*. Beijing: China University of Geosciences (M.S. thesis): 1–58.
- Zhang Shoucheng and Zhao Yan, 2016. Geological features of the Jiaochong Au-S ore deposit in Tongling and its further ore-prospecting potential. *Geology of Anhui*, 26(2): 99–103 (in Chinese with English abstract).
- Zhang Zhihui, 2009. *Study of the geological characteristic, ore-controlling conditions and genesis for the Jiaochong Au-S ore deposition in Tongling areas, Anhui Province*. Beijing: China University of Geosciences (M.S. thesis): 1–73.
- Zhang Zhihui, Zhang Da, Di Yongjun, Shu Bin, Pang Zhenshan, Du Zezhong, Que Chaoyang, Ma Xianping and Xue Jianling, 2013. Sulfur, lead isotope composition characteristics of the Jiaochong Au-S ore deposit in Tongling area and their indication significance. *Geological Bulletin of China*, 32(10): 1643–1652 (in Chinese with English abstract).
- Zhang, Y., Shao, Y.J., Li, H.B., and Liu, Z.F., 2017. Genesis of the Xinqiao Cu–Au–S deposit in the Middle-Lower Yangtze River Valley metallogenic belt, Eastern China: Constraints from U–Pb–Hf, Rb–Sr, S, and Pb isotopes. *Ore Geology Reviews*, 86: 100–116.
- Zhao Bin, 1989. *Main skarns and skarn deposits in China*. Beijing: Sciences Press, 268 (in Chinese with English abstract).
- Zheng Zejun, Du Yangsong, Lu Yinghuai, Chen Linjie, Yang Heming, Zhang Yun, Ren Chulei and Jiang Yongwei, 2015. Fluid mineralization process of hucunnao Cu–Mo deposit, Tongling, Anhui Province. *Mineral Deposits*, 34 (4): 692–710 (in Chinese with English abstract).
- Zhong Guoxiong, Zhou Taofa, Yuan Feng, Jiang Qisheng, Fan Yu, Zhang Dayu and Huang Jianman, 2014. LA-ICPMS U–Pb zircon age and molybdenite Re–Os dating of Yaojialing large zinc–gold polymetallic deposit, Tongling, Anhui Province, China. *Acta Petrologica Sinica*, 30(4): 1075–1086 (in Chinese with English abstract).
- Zhou Taixi, Chen Jiangfeng, Li Xueming and Foland, K.A., 1988. Has the Indo-sinian magmatism occurred in Anhui Province. *Acta Petrologica Sinica*, 4(3): 385–389 (in Chinese with English abstract).
- Zhou Taofa, Yuanfeng, Fanyu, Xie Jiancheng and Zhangxin, 2009. *A practical approach for ore deposits in Tongling ore concentration area*. Beijing: Geological Publishing House, 139 (in Chinese).
- Zhou Taofa, Zhang Lejun, Yuan Feng, Fan Yu and Cooke, D., 2016. LA-ICP-MS in situ trace element analysis of pyrite from the Xinqiao Cu–Au–S deposit in Tongling, Anhui, and its constraints on the ore genesis. *Earth Science Frontiers*, 17: 306–319 (in Chinese with English abstract).
- Zhou Taofa., Fan Yu, Yuan Feng and Zhong Guoxiong, 2012. Progress of geological study in the Middle-Lower Yangtze River Valley metallogenic belt. *Acta Petrologica Sinica*, 28: 3051–3066 (in Chinese with English abstract).
- Zhou Zhen, 1984. Research of the genesis of the Mashan gold deposit in Tongling, southern Anhui. *Geological Review*, 30 (5): 467–476 (in Chinese with English abstract).
- Zhou, T.F., Wang, S.W., Fan, Y., Zhang, D.Y., and White, N.C., 2014. A review of the intracontinental porphyry deposits in the Middle-Lower Yangtze River Valley metallogenic belt, Eastern China. *Ore Geology Reviews*, 65 (1): 433–456.
- Zuo Xiaomin, 2015. *Geology and ore-forming fluid geochemistry of the Guihuachong copper deposit, Anhui Province*. B China University of Geosciences (M.S. thesis): 1–54.

About the first author



FU Zhongyang, male; was born in 1992 in Zhoushan City, Zhejiang Province; Ph.D candidate of School of Resources and Environmental Engineering, Hefei University of Technology, Hefei. He is now interested in mineralogy, petrology, mineral deposit geology. Email: fuzhongyang824@sina.com. Phone: 15005607281.

About the corresponding author



XU Xiaochun, male; was born in 1961 in Qianshan City, Anhui Province; Professor of School of Resources and Environmental Engineering, Hefei University of Technology, Hefei. He is now interested in mineralogy, petrology, mineral deposit geology. Email: xuxiaoch@sina.com. Phone: 139666 53435.